Article

Molecular Cell

Acetylation of PCNA Sliding Surface by Eco1 Promotes Genome Stability through Homologous Recombination

Graphical Abstract

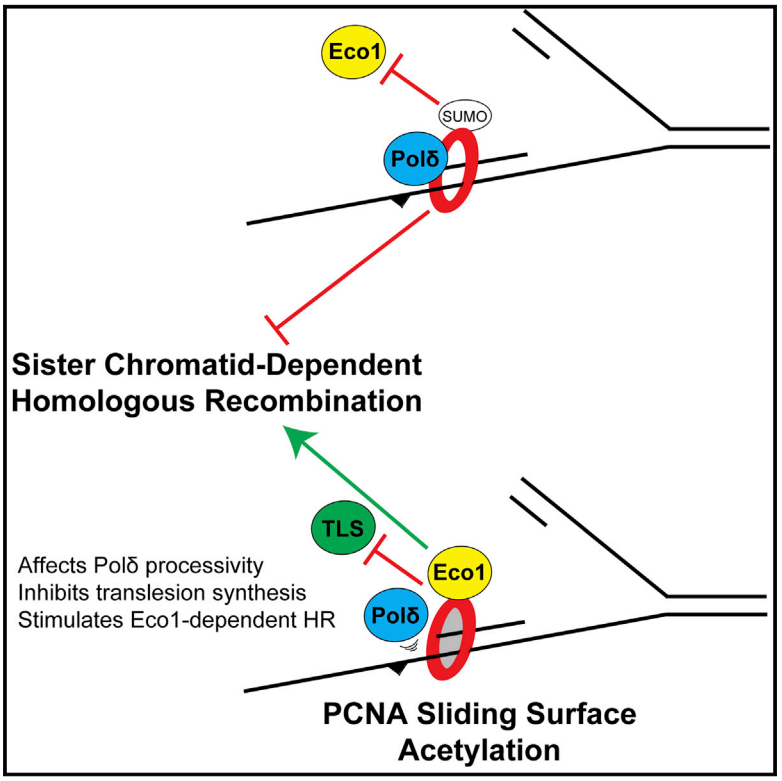

Highlights

- The PCNA ring is acetylated at its sliding surface in response to DNA damage
- Eco1, the cohesin-associated acetyltransferase, targets PCNA on lysine 20
- PCNA-K20ac suppresses DNA damage sensitivity of mutations in tolerance pathways
- PCNA-K20ac ring shows structural differences and stimulates homologous recombination

Authors

Pierre Billon, Jian Li,
Jean-Philippe Lambert, ...,
Tomohiko Sugiyama,
Jean-Francois Couture, Jacques Côté

Correspondence

jacques.cote@crhdq.ulaval.ca

In Brief

Billon et al. identify lysine acetylation as a regulatory modification at the inner surface of proliferative cell nuclear antigen (PCNA). DNA damage induces Eco1-mediated acetylation of PCNA at lysine 20, which stimulates repair by sister-chromatid-mediated homologous recombination.

Billon et al., 2017, Molecular Cell *65*, 78–90
January 5, 2017
http://dx.doi.org/10.1016/j.molcel.2016.10.033

CellPress

Molecular Cell
Article

Acetylation of PCNA Sliding Surface by Eco1 Promotes Genome Stability through Homologous Recombination

Pierre Billon,[1,8] Jian Li,[2] Jean-Philippe Lambert,[3] Yizhang Chen,[2] Véronique Tremblay,[4] Joseph S. Brunzelle,[5] Anne-Claude Gingras,[3,6] Alain Verreault,[7] Tomohiko Sugiyama,[2] Jean-Francois Couture,[4] and Jacques Côté[1,9,*]

[1]St-Patrick Research Group in Basic Oncology, Laval University Cancer Research Center, Centre de Recherche du CHU de Québec-Axe Oncologie, Quebec City, QC G1R 3S3, Canada
[2]Department of Biological Sciences and Molecular and Cellular Biology Graduate Program, Ohio University, Athens, OH 45701, USA
[3]The Lunenfeld-Tanenbaum Research Institute at Mount Sinai Hospital, Toronto, ON M5G 1X5, Canada
[4]Ottawa Institute of Systems Biology, Department of Biochemistry, Microbiology, and Immunology, University of Ottawa, 451 Smyth Road, Ottawa, ON K1H 8M5, Canada
[5]Department of Molecular Pharmacology and Biological Chemistry, Feinberg School of Medicine, Northwestern University, Chicago, IL 60611, USA
[6]Department of Molecular Genetics, University of Toronto, Toronto, ON M5S 1A8, Canada
[7]Institute for Research in Immunology and Cancer and Département de Pathologie et Biologie Cellulaire, Université de Montréal, Montreal, QC H3C 3J7, Canada
[8]Present address: Department of Genetics and Development, Herbert Irving Comprehensive Cancer Center, Columbia University Medical Center, New York, NY 10032, USA
[9]Lead Contact
*Correspondence: jacques.cote@crhdq.ulaval.ca
http://dx.doi.org/10.1016/j.molcel.2016.10.033

SUMMARY

During DNA replication, proliferating cell nuclear antigen (PCNA) adopts a ring-shaped structure to promote processive DNA synthesis, acting as a sliding clamp for polymerases. Known posttranslational modifications function at the outer surface of the PCNA ring to favor DNA damage bypass. Here, we demonstrate that acetylation of lysine residues at the inner surface of PCNA is induced by DNA lesions. We show that cohesin acetyltransferase Eco1 targets lysine 20 at the sliding surface of the PCNA ring in vitro and in vivo in response to DNA damage. Mimicking constitutive acetylation stimulates homologous recombination and robustly suppresses the DNA damage sensitivity of mutations in damage tolerance pathways. In comparison to the unmodified trimer, structural differences are observed at the interface between protomers in the crystal structure of the PCNA-K20ac ring. Thus, acetylation regulates PCNA sliding on DNA in the presence of DNA damage, favoring homologous recombination linked to sister-chromatid cohesion.

INTRODUCTION

During duplication of the genome, DNA is persistently under attack from endogenous and exogenous damaging agents (Ciccia and Elledge, 2010). Unrepaired lesions represent a challenge for chromosomal replication, which may lead to replisome stalling (Zeman and Cimprich, 2014). One strategy to overcome this is to restart DNA synthesis by a specialized class of DNA polymerases called translesion synthesis (TLS) polymerases, temporarily replacing the replicative polymerase (Sale, 2013). DNA polymerases are controlled by the processivity factor PCNA (proliferating cell nuclear antigen), which stimulates and restricts their activities (Moldovan et al., 2007). As part of the core mechanism of DNA synthesis, PCNA has a central role in replication and damage tolerance pathways, which are finely regulated by its posttranslational modifications (PTMs) (Hoege et al., 2002; Pfander et al., 2005; Stelter and Ulrich, 2003).

PCNA belongs to the family of DNA sliding clamps that adopt a special structure highly conserved in all organisms from bacteria to human (Kelman and O'Donnell, 1995). It has a ring-shaped homo-trimer structure that encircles DNA and allows sliding along the double-stranded helix (Georgescu et al., 2008; Krishna et al., 1994). PCNA sliding and its topological link to DNA confer high processivity to polymerases for DNA synthesis during replication and repair (Moldovan et al., 2007). Therefore, PCNA is organized into two functional interfaces. The external surface of the ring is implicated in the recruitment of various effectors along the genome (Mailand et al., 2013), while the central channel of the clamp is lined with an inner positively charged surface formed by four α helices. These helices associate with DNA to control PCNA sliding and efficient DNA synthesis (Ivanov et al., 2006). In spite of the importance of this surface in mediating DNA polymerase activity (Fukuda et al., 1995), the expected highly dynamic interaction between DNA and the sliding surface remains poorly understood (Ivanov et al., 2006).

PCNA is the master coordinator of DNA transactions at moving replication forks by acting as a docking platform to

recruit diverse functional partners (Mailand et al., 2013; Moldovan et al., 2007). The number of these partners is increased by PTMs located at the external surface of PCNA that modify the surface of interaction without changing the structure of the ring (Dieckman et al., 2012; Tsutakawa et al., 2015). One of these partners, the cohesin acetyltransferase Eco1, follows the replication fork to establish sister-chromatid cohesion during S phase through its direct binding to PCNA (Lengronne et al., 2006; Moldovan et al., 2006; Rolef Ben-Shahar et al., 2008; Unal et al., 2008). The interaction between Eco1 and PCNA is counteracted by PCNA-SUMOylation (Moldovan et al., 2006), a modification required to control DNA damage bypass pathways (Branzei and Foiani, 2010; Mailand et al., 2013). Eco1 and sister chromatids are critical for repair because cohesion established during S phase stimulates homologous recombination (HR) (Sjögren and Ström, 2010).

Here, we describe an unexpected regulation of PCNA sliding surface through acetylation. Interestingly, this modification is induced by DNA damage and is important for genome stability. We demonstrate that Eco1 is responsible for acetylation of a specific lysine, K20, which in turns stimulates HR. This leads to striking suppression of the DNA damage sensitivity of cells carrying mutations in damage tolerance pathways. Finally, we report the crystal structure of the PCNA ring acetylated on K20, which reveals structural differences at the interface between PCNA subunits. Altogether, our observations open new conceptual perspectives on the mechanisms of PCNA sliding on the DNA to regulate polymerases, raising unexpected insights into PCNA as a processivity factor.

RESULTS

DNA Damage-Induced Acetylation of PCNA Inner Surface Is Important for Cell Survival

The internal surface of the sliding-clamp PCNA is positively charged, creating favorable electrostatic contact with the negatively charged DNA (Kelman and O'Donnell, 1995; Krishna et al., 1994) (Figure 1A). It is noteworthy that the positive lysine and arginine residues lining the internal surface of the sliding clamp are highly conserved throughout evolution. The lysine/arginine ratio is also conserved since there are six lysine and three arginine residues in both higher and lower eukaryotes (Figure 1B). In addition, the exact positions of several lysines (K13, K20, K77, and K217) are strictly conserved. These observations suggest that the nature and position of these lysine residues are important for PCNA function.

Since PCNA controls the processivity of different polymerases at DNA lesions, we hypothesized that the requirement for PCNA sliding might be different on normal DNA compared to damaged templates. To explore whether the basic internal surface of PCNA is modulated when DNA lesions block sliding, we compared the electrophoretic mobility of PCNA from budding yeast (Pol30) on an isoelectric focusing gel (2D gel). Remarkably, we observed that after treating cells with a DNA-damaging agent (methyl methanesulfonate, MMS), a portion of PCNA molecules became more acidic compared to untreated cells (Figure 1C). This MMS-induced appearance of acidic molecules might result from a high level of PTMs, as observed for human PCNA (Naryzhny and Lee, 2004). We then mutated the six internal lysine residues into arginines (K13R, K20R, K77R, K146R, K210R, and K217R) to generate a PCNA mutant named Pol30-6KR. Importantly, this mutant does not produce the same population of acidic PCNA molecules upon MMS treatment (Figure 1C). Therefore, we investigated whether PTMs of these highly conserved lysine residues were previously mapped on PCNA in large-scale mass spectrometry studies and found that, indeed, certain sites were found to be acetylated in yeast (Henriksen et al., 2012), rat (Lundby et al., 2012), and human cells (Cazzalini et al., 2014; Chen et al., 2012; Choudhary et al., 2009) (Table S1, available online). To test whether PCNA is acetylated in response to DNA damage, we performed immunoprecipitations of acetylated proteins from whole-cell extracts. While a fraction of PCNA was immunoprecipitated in all conditions, a much larger portion was specifically obtained with the extract derived from MMS-treated cells (Figure 1D). Furthermore, mass spectrometry analysis of purified yeast PCNA revealed multiple acetyl-lysine residues at the sliding surface of PCNA after MMS exposure (Table S1; Figure S1A). Importantly, we identified several peptides containing acetylated lysine 20 (K20ac) (Figure 1E). This acetylated lysine had not been detected in previous large-scale mass spectrometry studies (Table S1), suggesting that PCNA acetylation on K20 may have a specific function in response to DNA damage.

To investigate the function of acetylation on the lysine residues lining the internal surface of the PCNA ring, we first looked at the phenotype of mutant cells expressing non-acetylatable Pol30-6KR. Intriguingly, these cells are fully viable, with no growth defect in normal media, indicating normal replicative function of the mutant PCNA molecule (Figure S1B). In contrast, mutant cells expressing Pol30-6KR display specific sensitivity to MMS, but not hydroxyurea (Figures 1F and S1C), and we observed that viability was significantly compromised upon short exposure to MMS (Figure 1G). This supports the idea that acetylation of the lysine residues at the inner surface of the ring is required during replication of damaged DNA templates. At this point, it is tempting to speculate that acetylation in the center of the PCNA ring, which neutralizes the positive charges of the lysine residues, drastically affects its electrostatic potential to regulate the dynamic sliding of PCNA on damaged templates.

Intricate Regulation of PCNA Inner Surface for Genome Stability

In order to further explore the role of PCNA acetylation, we substituted individual conserved lysine residues of the sliding surface with an acetyl-mimic glutamine residue and determined that each single mutant is viable and exhibits normal growth (Figures S2A–S2C). Since acetylation of PCNA increases in response to MMS, we tested whether cells carrying the single glutamine substitutions are sensitive to the drug. While most point mutants do not show sensitivity, cells expressing the K20Q substitution show a marked growth defect in the presence of MMS (Figure 2A). The Pol30-K77Q mutant is also sensitive to a lesser extent, while both mutants are not significantly sensitive to hydroxyurea (Figure S2D). Cell survival assays in liquid culture also show severely reduced viability after short exposure to

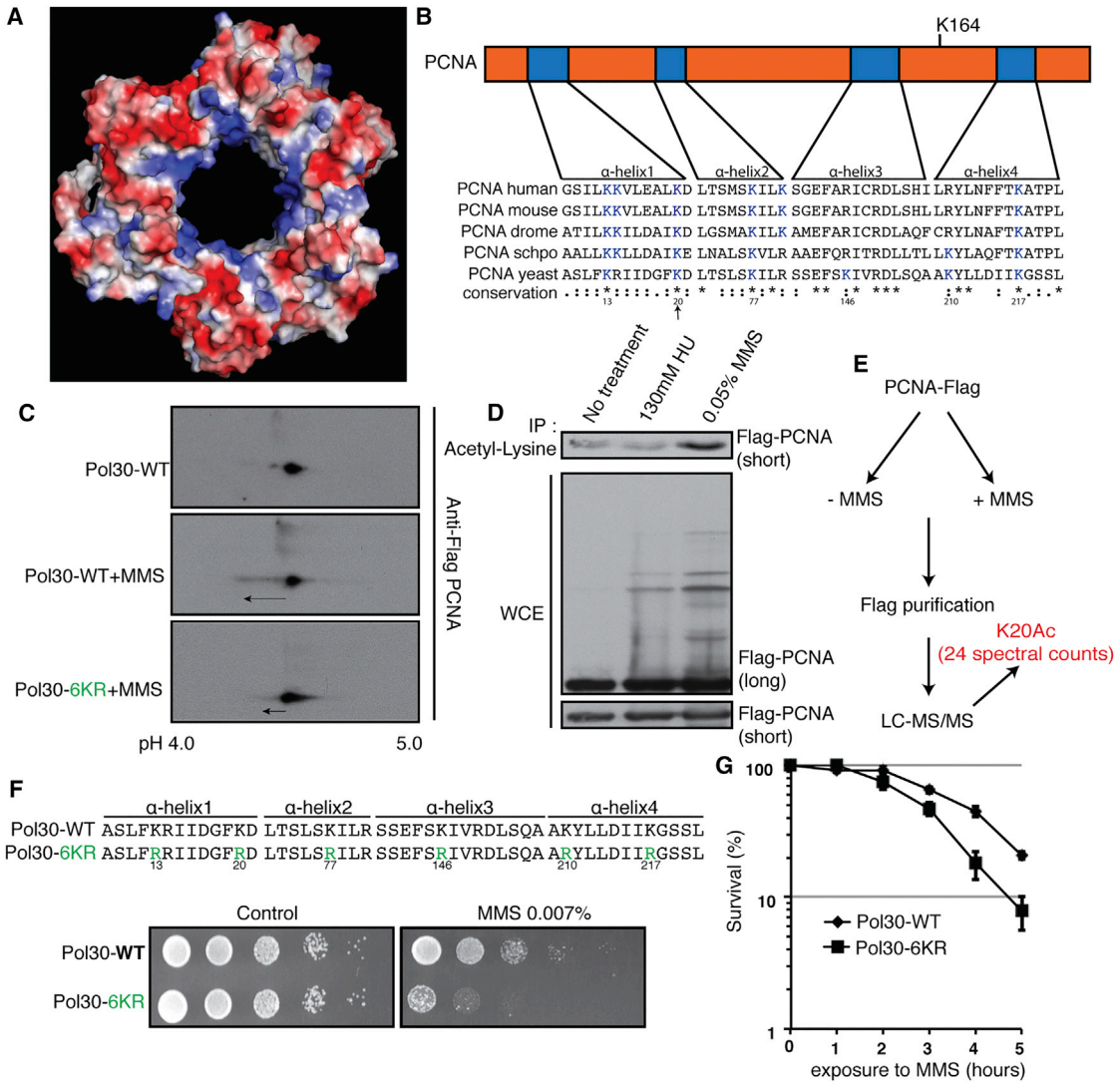

Figure 1. DNA Damage-Induced Acetylation of PCNA Sliding Surface Is Important for Cell Survival

(A) Visualization of the PCNA ring electrostatic potential (based on PDB: 3K4X; McNally et al., 2010), revealing the strongly positive inner surface. Blue, positive; red, negative.

(B) Sequence alignment of four PCNA inner α helices that contact DNA, from lower eukaryotes to human, using ClustalW (http://www.ebi.ac.uk/Tools/msa/clustalw2). This highlights the strict conservation of lysines at positions 13, 20, 77, and 217. The six lysines present in each organism are in blue. (*) conserved residue, (:) similar residues, (.) weakly similar residues. drome, *Drosophila melanogaster*; schpo, *Schizosaccharomyces pombe*; yeast, *Saccharomyces cerevisiae*.

(C) Cells expressing Flag-Pol30-WT or Flag-Pol30-6KR mutant were treated with or without 0.05% MMS for 2 hr. Cell extracts were loaded in parallel on 2D isoelectric focusing gels (pH 4–7 and 12% SDS-PAGE) and analyzed by western blot with anti-Flag antibody. Arrows show the acidification of PCNA upon incubation of cells with MMS, a change suppressed by the substitution of the six lysines at the inner surface of PCNA to arginines.

(D) G1-blocked cells were released in yeast peptone dextrose (YPD) containing either 0.05% MMS or 130 mM hydroxyurea (HU) for 2 hr, or for 15 min with no drug (no treatment). Cell extracts were immunoprecipitated with an anti-acetylated lysine antibody. PCNA was then detected by western blot using anti-Flag, revealing a strong enrichment of acetylated PCNA in the MMS-treated extract. WCE, whole-cell extract.

(E) Flag-tagged PCNA was purified from cells treated with or without 0.05% MMS and analyzed by tandem mass spectrometry of tryptic peptides to detect PTMs. Liquid chromatography-tandem mass spectrometry (LC-MS/MS) analysis identified several peptides containing K20ac in MMS-treated samples.

(F) Substitution of six PCNA inner lysines to charge-preserving arginines creates no growth defect but leads to DNA damage sensitivity. Sequence of PCNA four α helices shows the six K to R substitutions in the Pol30-6KR mutant used in spot assay. A 10-fold serial dilution of the wild-type and mutant cells was spotted on control or MMS-containing plates.

(G) Survival curve of the Pol30-6KR mutant compared to wild-type cells upon increasing time of exposure to 0.2% MMS-containing media. Error bars indicate SEM of three independent experiments.

See also Figure S1.

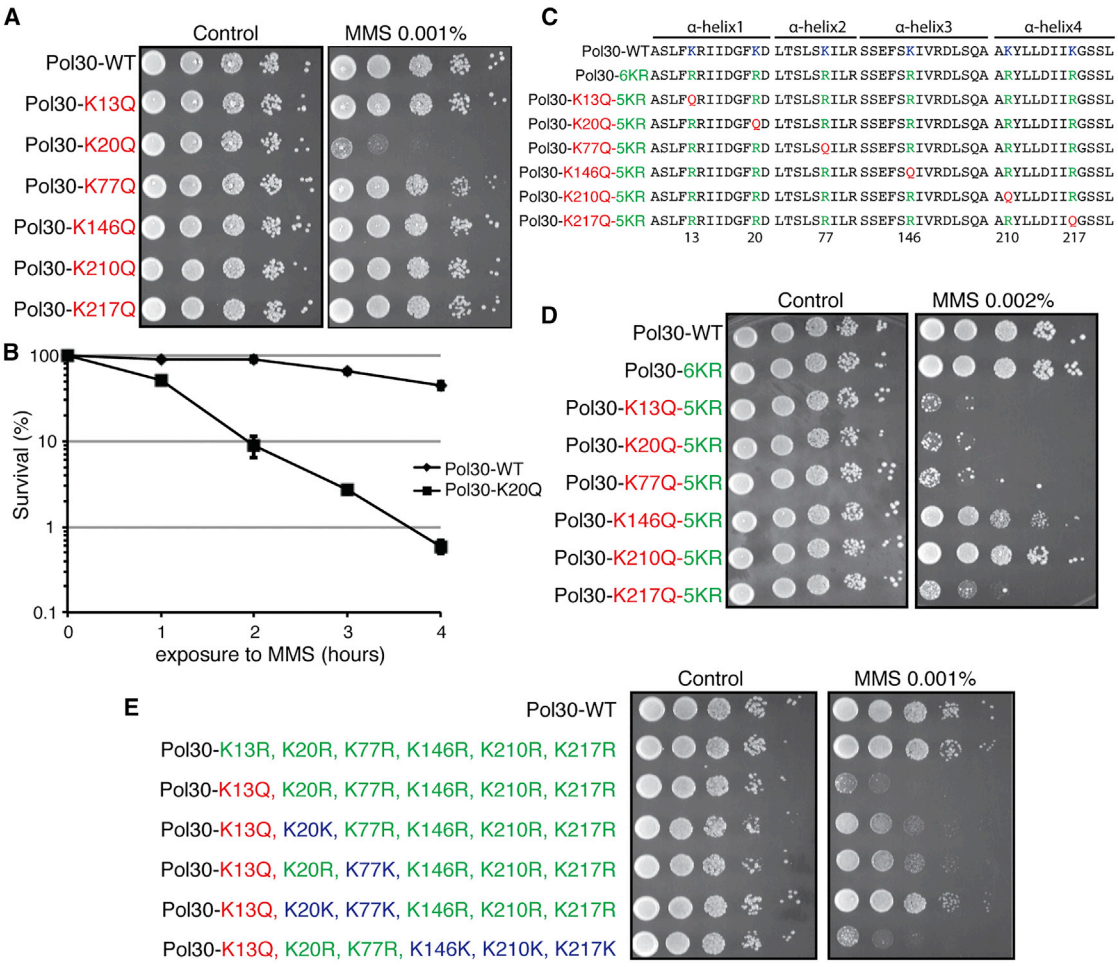

Figure 2. Intricate Regulation of the Acetylated Lysines at the Inner Surface of PCNA Ring Controls Resistance to DNA Damage

(A) DNA damage sensitivity assay of strains containing the indicated individual acetyl-mimic substitution mutant (K to Q). Serial dilutions of the indicated cells were spotted on control or MMS-containing plates.

(B) Survival curve of Pol30-K20Q mutant compared to wild-type cells after increasing time of exposure to 0.2% MMS. Error bars represent SEM of independent triplicates.

(C) Sequence of the different combinations of substitutions in the four α helices used in DNA damage sensitivity assays in (D).

(D) Spot test for the indicated mutants shows the hypersensitivity to MMS of cells with the strictly conserved lysines substituted for acetyl-mimic glutamine, while the other lysines are mutated in charge-preserving non-acetylatable arginines.

(E) Serial dilution of indicated mutant cells on control and MMS plates reveals the suppression of DNA damage sensitivity of the Pol30-K13Q-5KR mutant by reintroducing a lysine at positions K20 and K77.

See also Figure S2.

MMS (Figures 2B and S2E), and viability is mainly compromised with treatment restricted to S phase (Figure S2F). The absence of phenotypes for the other acetyl-mimic mutants was surprising since these lysine residues were found acetylated in vivo. Therefore, PCNA could be regulated by intricate and partially redundant cycles of acetylation/deacetylation at the inner surface of the ring, controlling its sliding for DNA damage resistance. To remove potential redundancy, we mutated all the lysine residues of the internal α helices to arginine while one position remained substituted by glutamine (Figure 2C). Strikingly, single acetyl-mimic mutants on K13, K20, K77, and K217 are hypersensitive to MMS when the five other lysine positions remain fixed as positively charged arginine residues (Figure 2D). This indicates that acetylation/deacetylation on the other lysine residues is also important for cellular resistance to MMS. Importantly, reintroducing a lysine at positions 20 and 77 rescues the strong MMS sensitivity observed for the Pol30-K13Q-5R mutant (Figure 2E). This rescue implies that it is dependent on a PTM of the lysine residue. It is noteworthy that K13, K20, K77, and K217 are the only internal lysines strictly conserved in eukaryotes (Figure 1B), emphasizing the importance of their acetylation for cellular resistance to MMS. This detailed in vivo mutagenesis and phenotypic analysis of PCNA sliding surface uncovers an unexpected new regulatory mechanism.

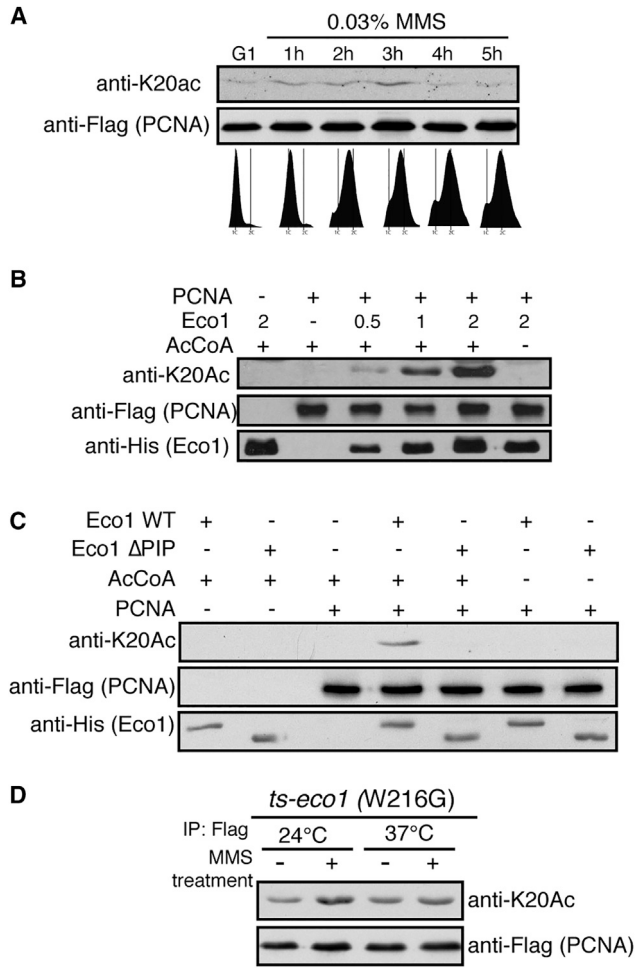

Figure 3. PCNA Is Acetylated by Eco1 Both In Vitro and in Response to DNA Damage In Vivo

(A) Cell-cycle regulation of K20ac was monitored in the presence of DNA damage. Wild-type cells expressing 2Flag-PCNA were released from G1 into the cell cycle for the indicated times in presence of 0.03% MMS. PCNA was immunoprecipitated followed by western blot for K20ac detection and correlated with cell-cycle profiles.

(B) In vitro acetylation assay of PCNA using purified His-Eco1 acetyltransferase shows specific acetylation of K20. The indicated acetylation reactions were analyzed by western blot using anti-K20Ac antibody. Detection of PCNA acetylated on K20 requires Eco1 and acetyl-CoA.

(C) In vitro acetylation of PCNA using purified Eco1 and Eco1 lacking its PIP box. Wild-type and mutant GST-Eco1 recombinant proteins were used in order to clearly separate PCNA and Eco1-ΔPIP after gel migration.

(D) The MMS-induced acetylation of PCNA is lost at restrictive temperature. ts-*eco1* mutant cells expressing 2Flag-PCNA were synchronized in G1 at 24°C and were then put at 37°C or 24°C for 3 additional hours in G1. Cells were then released in S phase with 0.03% MMS for 2 hr or in normal S phase for 15 min. See also Figure S3.

Cohesin Acetyltransferase Eco1 Targets PCNA on Lysine 20

Intrigued by the strong phenotype of cells expressing Pol30-K20Q (Figure 2A), we raised an antibody against PCNA K20Ac to study its regulation (Figures S3A and S3B). First, we observed that acetylation of PCNA K20 increases in response to MMS during S phase (Figures 3A and 3D) but remains unchanged throughout the cell cycle in absence of damage (Figure S3C). These data suggest that PCNA acetylation is linked with DNA synthesis upon DNA damage, consistent with the specific phenotype observed with MMS. In order to identify the enzyme responsible for PCNA acetylation at K20, we used a candidate approach to perform in vitro acetyltransferase assays with purified enzymes and substrates (Figures S3D–S3G). We tested the NuA4 and Rtt109/Vps75 histone acetyltransferase complexes and the cohesin acetyltransferase Eco1 since these were previously shown to functionally interact with PCNA, and it was specifically Eco1 that demonstrated direct physical interaction to promote sister-chromatid cohesion (Collins et al., 2007; Moldovan et al., 2006; Renaud-Young et al., 2015). Interestingly, only incubation of Eco1 with PCNA and acetyl-CoA produces a signal detected by the anti-K20ac antibody (Figures 3B and S3G), indicating that Eco1 is able to transfer acetyl groups on PCNA K20. Importantly, Eco1-dependent acetylation of PCNA depends on the interaction mediated by Eco1 PCNA-interacting peptide (PIP) (Figure 3C), even though wild-type and ΔPIP enzymes have similar enzymatic activities per se (Moldovan et al., 2006). The analysis of this reaction by mass spectrometry not only confirmed K20ac, but also demonstrated acetylation of other lysines at the inner surface of the ring (Figure S3H). Next, we analyzed if PCNA acetylation on K20 was indeed regulated by Eco1 in vivo using thermosensitive (ts) *eco1* mutant cells. While the basal level of K20ac seems unaffected in these cells, we observed that the MMS-induced acetylation is specifically lost at restrictive temperature (Figure 3D), implicating Eco1 for the acetylation of PCNA in vivo upon MMS exposure. Together, these results point toward a function of Eco1-dependent acetylation of PCNA in response to DNA damage. Importantly, this concurs with observations that mutations in Eco1 acetyltransferase activity lead to sensitivity to agents that induce replication fork stalling and DNA repair defects (Gordillo et al., 2008; Lu et al., 2010), and affect DNA synthesis/fork processivity (Terret et al., 2009).

PCNA K20Ac Stimulates Cohesion-Mediated HR and Suppresses the MMS Sensitivity of Mutations in DNA Damage Tolerance Pathways

Since it was shown that PCNA recruits Eco1 to replication forks to promote sister-chromatid cohesion during S phase (Moldovan et al., 2006) and because HR preferentially uses sister chromatids to repair DNA lesions, we examined how PCNA acetylation affects DNA damage tolerance pathways at replication forks, namely damage bypass by TLS or template switching. These pathways are dependent on modifications of the PCNA ring on residue K164 located on its external surface (Branzei and Foiani, 2010; Mailand et al., 2013). They include PCNA mono- and polyubiquitination by Rad6/Rad18-Rad5 to promote damage bypass and SUMOylation by Siz1 to block the formation of cytotoxic recombination intermediates (Hoege et al., 2002; Mailand et al., 2013; Papouli et al., 2005; Pfander et al., 2005). We observed that while a PCNA mutant that cannot be modified on K164 (Pol30-K164R) is highly sensitive to MMS, to a similar extent as our Pol30-K20Q single mutant, combination of both mutants in the same molecule strongly suppresses their MMS

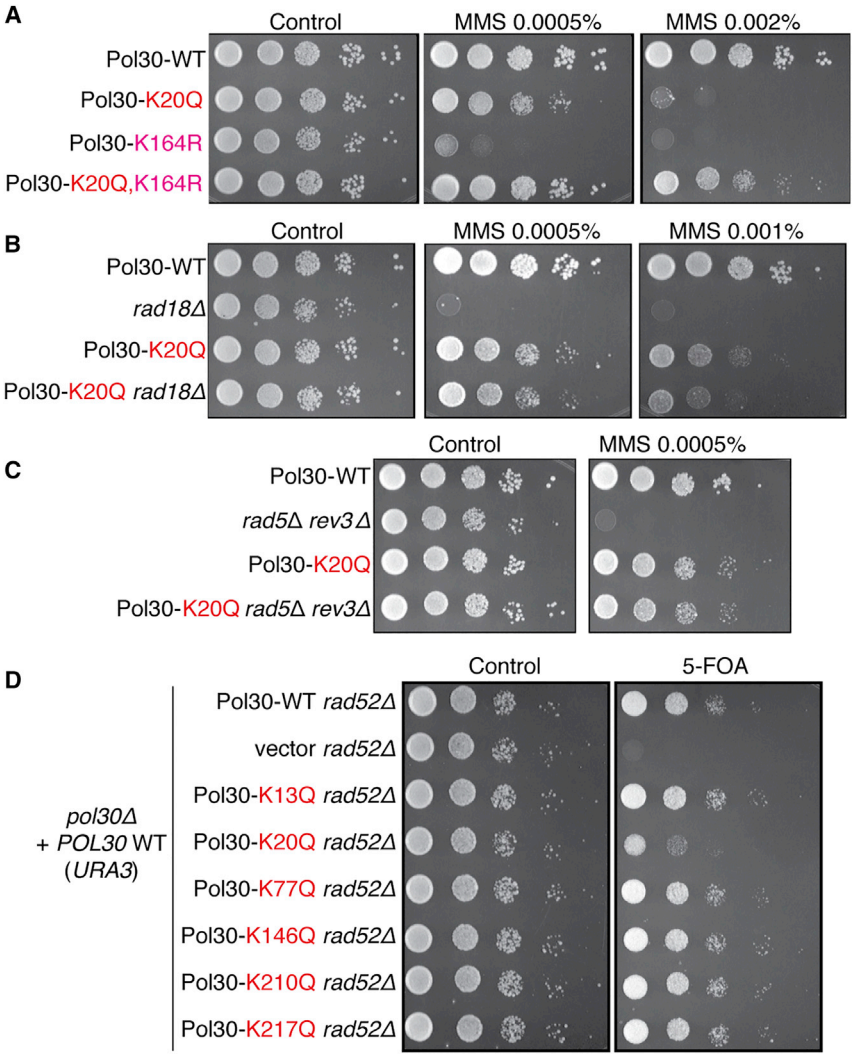

Figure 4. PCNA Acetylation Robustly Suppresses DNA Damage Sensitivity of Mutants in the Damage Tolerance Pathway

(A) Serial dilution spot assay to demonstrate the functional interaction between *pol30-K20Q* and *pol30-K164R* mutations. The high sensitivity to MMS of cells expressing each mutant is suppressed when the mutations are combined.

(B and C) The *pol30-K20Q* allele (B) also strongly suppresses the DNA damage sensitivity of *rad18* and (C) *rev3 rad5* double-mutant cells.

(D) Plasmid shuffle experiment demonstrating the genetic interaction between HR and PCNA acetylation on K20. Serial 10-fold dilution of *rad52Δ pol30Δ* cells expressing *POL30*-WT on *URA3* plasmid and the indicated *pol30* mutants from a *TRP1* vector were spotted on control plates or in the presence of 5-FOA to remove the URA3 vector. Rad52 is required for normal growth in cells expressing Pol30-K20Q.

See also Figure S4.

sensitivities (Figure 4A). This is linked to at least some aspect of the PCNA ubiquitination pathway, for Pol30-K20Q robustly suppresses the MMS sensitivity of *rad18*Δ and *rad6*Δ mutant cells (Figures 4B and S4A). Further dissection of the two damage-bypass pathways, TLS (*Rad30/Rev3*) and template switching (*Rad5*), also confirms suppression of MMS sensitivity by the Pol30-K20Q mutant (Figures 4C, S4B, and S4C). Furthermore, the MMS sensitivity of Pol30-K20Q is partially suppressed by loss of Siz1 (Figure S4D), recapitulating the reciprocal suppression seen in the K164R-K20Q double mutant and linking K20 acetylation to HR mechanisms. Based on these data and because Eco1-dependent sister-chromatid cohesion stimulates HR to repair DNA lesions, we speculated that HR-dependent replication fork salvage might be the only pathway available in the acetylation-mimic PCNA mutant. Therefore, we tested the viability of each single acetyl-mimic mutant in an HR-deficient background and observed that Pol30-K20Q is synthetically sick with *rad52*Δ, for double-mutant cells show a significantly increased doubling time even in the absence of a DNA damaging agent (Figures 4D, S4E, and S4F).

To better understand whether these striking phenotypes are specifically due to the acetylation of K20, we have mutated the residue to an alanine (Pol30-K20A), which does not mimic an acetyl-lysine while still losing the positive charge. Interestingly, cells expressing the Pol30-K20A mutant are significantly less sensitive to MMS than the ones with the Pol30-K20Q mutant (Figures 5A and 5B). This indicates that the simple loss of K20 positive charge does not recapitulate the K20Q phenotype and that acetylation must be regulated in order to achieve proper DNA damage resistance. Furthermore, we observed that *rad18* sensitivity to MMS is not suppressed by the Pol30-K20A mutant, in contrast to the robust suppression observed with the Pol30-K20Q mutant (Figure 5A). Again, this result implies a specific function of the acetylated lysine on PCNA inner surface, not simply the loss of the positive charge. We observed that this phenotype is specifically linked to the TLS pathway since the Pol30-K20A mutant suppresses the MMS sensitivity of *rad5* mutant cells, as does Pol30-K20Q, but is synthetically sick with *rad30* TLS polymerase mutant, unlike the glutamine substitution (Figures 5B and 5C). Importantly, analysis of purified PCNA K20Q and K20A mutants indicates a complete loss of SUMOylation (Figure 5D). Therefore, suppression of the MMS sensitivity of *rad5* mutant cells by both K20 substitutions may be a consequence of the absence of SUMO. On the other hand, the robust suppression of *rad18* and *rad6* MMS sensitivities by PCNA K20Q cannot be explained by the loss of SUMOylation since both K20Q and K20A substitutions lack SUMO. In addition, the strong suppression of PCNA-K164R MMS sensitivity by intragenic K20Q also demonstrates a SUMO-independent mechanism (since K164R lacks SUMO to begin with) (Figure 4A). Nevertheless, these findings suggest

that PCNA acetylation and SUMOylation have an antagonistic relationship. Indeed, SUMO-PCNA is known to prevent HR and to block Eco1 recruitment to the fork (Moldovan et al., 2006; Papouli et al., 2005; Pfander et al., 2005). Consistent with a specific role of acetylation in favoring HR, the Pol30-K20A mutant is not synthetically sick with *rad52* mutant cells, unlike K20Q (Figure 5E). The close functional link between PCNA acetylation on K20 and Eco1 is further supported by the observation that the overexpression of the Pol30-K20Q mutant increases the ts phenotype of *eco1* cells, while wild-type and PCNA mutants lacking SUMO suppress it (Moldovan et al., 2006) (Figures 5F and S4G). Finally, in agreement with the results above, we found that mimicking PCNA acetylation, not the simple loss of positive charge, strongly stimulates HR in vivo, and that this occurs even in an *siz1* mutant background lacking the SUMO ligase (Figures 5G, S4H, and S4I). Altogether, these data demonstrate that acetylation of PCNA by Eco1 specifically favors HR-dependent mechanisms through sister-chromatid cohesion to overcome the DNA lesions. Taken together, our data point toward a close relationship among Eco1 acetyltransferase, establishment of sister-chromatid cohesion, and PCNA sliding in modulating the response to DNA damage during S phase.

Acetylation of PCNA on K20 Specifically Affects the Processivity of Replicative DNA Polymerase δ

Since PCNA sliding is required to stimulate DNA polymerases by increasing their processivity (Chilkova et al., 2007; Fukuda et al., 1995; Ivanov et al., 2006; Kochaniak et al., 2009; Laurence et al., 2008), it was tempting to speculate that PCNA acetylation might control the activities of polymerases during DNA synthesis. This is consistent with the observation that the combined loss of multiple positive residues is lethal (data not shown). Neutralization of positive charges by acetylation might be a regulatory mechanism to control the activity of polymerases at DNA lesions. This regulation should be highly dynamic, for we could not detect any changes in protein levels, chromatin association, and co-immunoprecipitation of Polδ with our PCNA mutants (Figure S5A) (data not shown), in contrast to what has been proposed (Cazzalini et al., 2014; Yu et al., 2009). To test a possible function linked to sliding and polymerase processivity, we used a deletion mutant of the non-essential Polδ subunit Pol32. Disruption of the *POL32* gene results in instability during S phase, due to defects in polymerase processivity and formation of single-stranded DNA (ssDNA) gaps, observable by a growth defect at low temperatures (Johansson et al., 2004). The cold sensitivity of *pol32*Δ cells is significantly increased when combined with the *pol30*-K20Q mutant, consistent with a deficiency in replication fork processivity (Figure 6A). These observations support the possibility that the Pol30-K20Q mutant only affects Polδ in the presence of DNA damage; otherwise, an effect on normal DNA replication would lead to a lethal or slow growth phenotype. To directly measure the effect of Pol30-K20Q on Polδ activity, we compared the ability of PCNA mutants to stimulate DNA polymerases using purified proteins in vitro (Li et al., 2013) (Figure S5B). All PCNA molecules could be efficiently loaded onto DNA by the clamp loader, and primer extension was initiated by addition of DNA polymerases. Polδ-dependent DNA synthesis is less efficient with the PCNA K20Q mutant because abortive intermediates are clearly detected (Figure 6B). This inhibition of DNA synthesis was observed using both ssDNA and recombination-like D-loop templates, as well as UV-irradiated DNA (data not shown). We also reproduced the negative effect on Polδ with a purified recombinant PCNA molecule that is fully acetylated on K20, indicating that the K20Q mutation efficiently mimics K20ac (Figures 6C and 6D). In contrast, the processivity of TLS polymerases Polη and Polζ is not affected by the Pol30-K20Q mutant (Figures S5C and S5D), supporting a specific role of PCNA K20ac to transiently modulate Polδ activity (Figures S5E–S5H). In addition to affecting sliding of the ring, acetylation of PCNA inner surface might represent a regulatory mechanism by which Polδ-dependent DNA synthesis can be modulated at DNA lesions. Further studies will be needed to define whether PCNA acetylation upon DNA damage stimulates HR in part by blocking the polymerase switch necessary for TLS.

Acetylation of PCNA Lysine 20 Is Linked to Structural Changes at the Interface between Protomers

We next sought to determine the impact of K20 acetylation on the structure of the PCNA ring. The crystal structure of $PCNA^{K20ac}$ at 3.27 Å (R_{free} of 20.7%; Table 1) reveals three molecules in the asymmetric unit. Similar to the unmodified PCNA, $PCNA^{K20ac}$ adopts the canonical ring-shaped structure in which the α helices lined the interior of the clamp and the β strands composed the exterior of PCNA (Figure 7A). Alignment of acetylated and unmodified PCNA structures reveals a root-mean-square deviation of 0.8, suggesting that K20 acetylation does not trigger large conformational changes (Figure 7B). Consistently, both α1 helices, containing the acetylation site, superpose well, demonstrating that acetylation does not change the orientation of the PCNA first α-helix. Interestingly, in the unmodified form of PCNA, K20 engages in polar contacts with Asp17 carboxylate groups and its backbone carbonyl group, neutralizing its side chain (Krishna et al., 1994). Alternatively, K20 was recently found to interact with Asp21 (in the case of a monomeric PCNA molecule bound by E2-E3-SUMO; Streich and Lima, 2016). In stark contrast, no electronic density can be detected for K20ac, indicating a high degree of mobility inside the ring compared to unmodified PCNA (Figures S6A and S6B). Further inspection of the aligned structures shows that while α1 helices superpose well, an extra turn can be observed on α2 of $PCNA^{K20ac}$ (Figure 7C). This turn places several residues, including R80 and C81, closer to residues found on the opposing protomer, including Q153 and D150 (Figures 7C and 7D). In addition, in contrast to the non-acetylated form of PCNA, this conformational change brings the backbone of α2 slightly closer to the other protomer (Figures 7E and 7F). Analogously, the C terminus of β8 and the β9 strand seem slightly shifted toward the other protomer in the $PCNA^{K20ac}$ ring (see also Figure S6C for electron densities). Interestingly, the affected interface between the protomers corresponds to the binding site of the Ubc9 subunit of the E2/E3(Siz1) complex that SUMOylates K164 (Streich and Lima, 2016). In addition, the loop J (aa 105–110) is disorganized between residues 108 and 110 in $PCNA^{K20ac}$. While clear conclusions about the disorganization of this loop are not possible at this level of resolution, it is interesting that this has been previously linked to defects in TLS, as

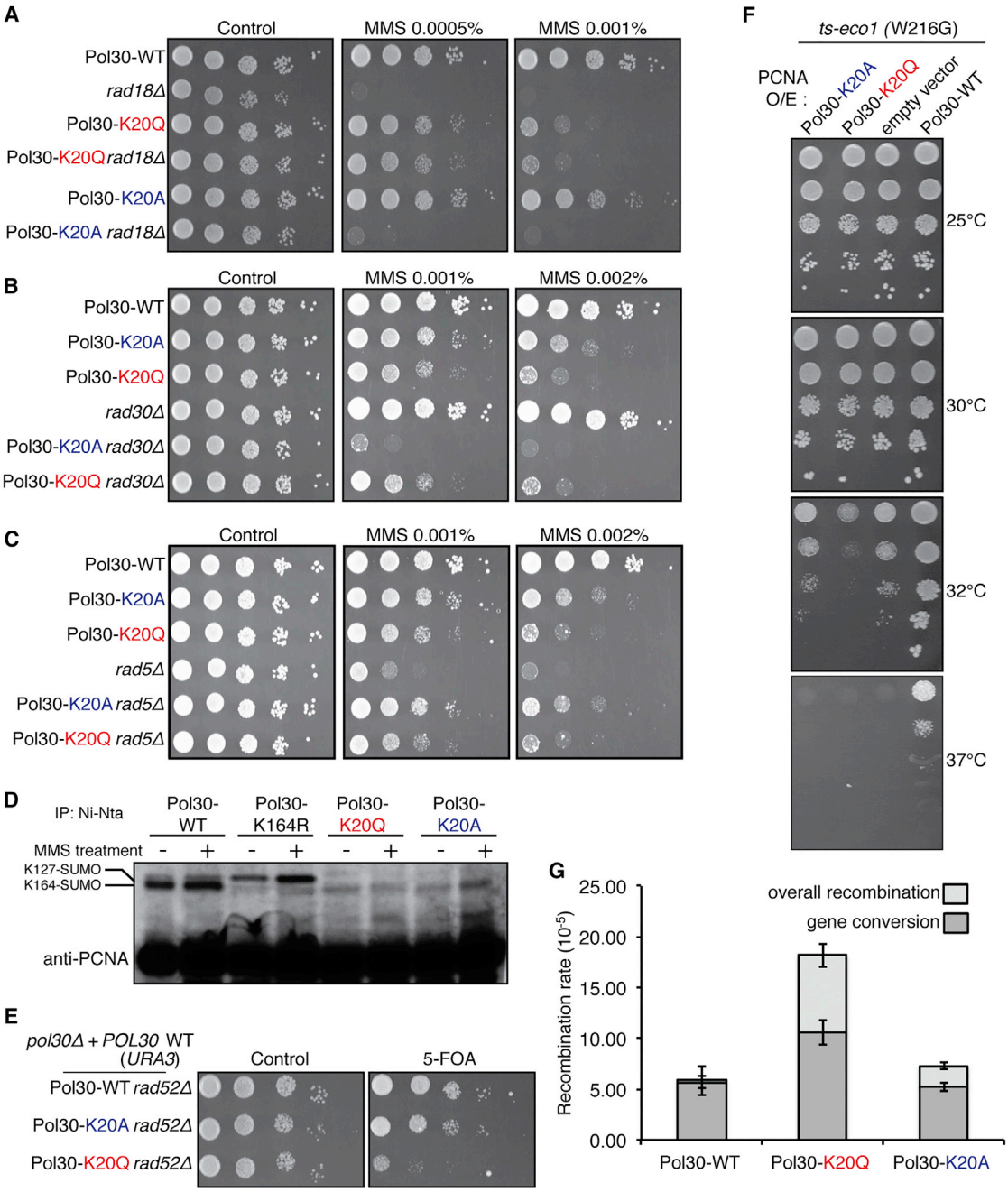

Figure 5. PCNA Acetylation on K20, Not the Loss of Positive Charge, Specifically Suppresses Defects in TLS and Stimulates HR

(A–C) Serial dilution spot assay to demonstrate distinct genetic interactions of *pol30-K20Q* and *pol30-K20A* mutants with components of the DNA damage bypass pathways, supporting a specific role of K20 acetylation in suppression of TLS. Suppression of *rad18* sensitivity to MMS is specific to K20Q (A), while K20A, but not K20Q, is synthetically sick on MMS with *rad30* TLS defective cells (B). In contrast, both K20Q and K20A alleles suppress MMS sensitivity of *rad5* template switching mutant (C).

(D) Loss of PCNA SUMOylation in cells expressing both Pol30-K20Q and Pol30-K20A. PCNA was purified in denaturing conditions using Ni-NTA resins to reveal SUMO modifications on K127 and K164 after gel migration and western blot analysis with anti-PCNA; cells expressing Pol30-K164R are shown as control.

(E) The synthetic growth defect produced by combining *pol30-K20Q* and *rad52*Δ mutants is not reproduced with the *pol30-K20A* allele. Plasmid shuffling and spot assays were performed as in (D).

(F) Overexpression of exogenous wild-type PCNA, K20Q, or K20A mutants shows opposing effects on the viability of *eco1* ts mutant cells. Cells carrying a normal chromosomal *POL30* allele and the *eco1-W216G* ts mutant were transformed with 2Flag-Pol30-WT, 2Flag-Pol30-K20Q, 2Flag-Pol30-K20A, or empty vector followed by spot assays at the indicated temperatures.

(legend continued on next page)

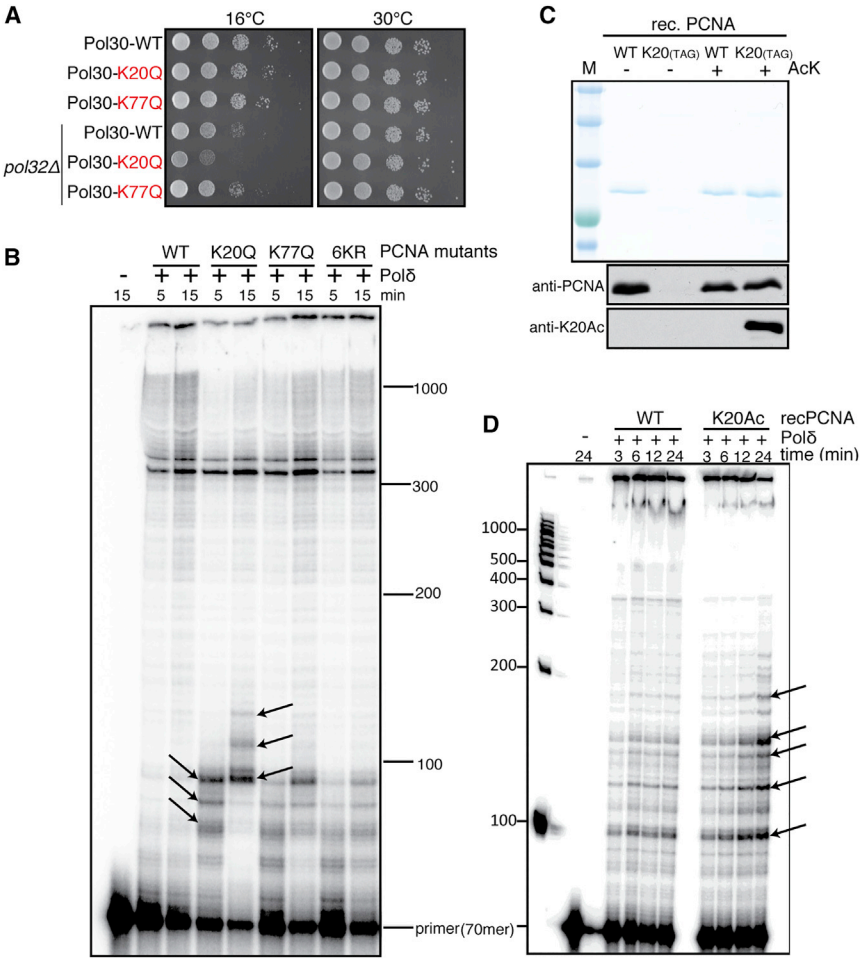

Figure 6. Constitutive Acetylation of PCNA K20 Leads to Polδ Processivity Defects

(A) Growth assay by serial dilution showing the functional interaction between PCNA acetylation at K20 (Pol30-K20Q) and DNA polymerase δ -processivity (Pol32). Single- and double-mutant cells were spotted on plates and incubated at the indicated temperature. Slower growth at low temperature is indicative of processivity defect.

(B) Polδ-dependent DNA synthesis is affected by the PCNA K20Q mutant in a purified in vitro reconstituted system. The indicated purified PCNA molecules were loaded onto DNA with the clamp loader complex (RFC) followed by extension of a 32P-labeled primer with Polδ for 5 or 15 min, and migration on a denaturing gel. Arrows indicate abortive extensions with the PCNA K20Q mutant.

(C) Coomassie staining showing the production of a fully acetylated recombinant PCNA specifically at K20. The lysine 20 codon has been replaced by the amber codon TAG. In presence of Nε-acetyllysine (AcK) and tRNA (CUA), the aminoacyl-tRNA synthetase allows the specific incorporation of AcK at K20 position, as confirmed by the western blot using the anti-K20ac antibody. Anti-PCNA blot is used as loading control.

(D) Polδ-dependent DNA synthesis is also affected by PCNA acetylated on K20, as observed with the K20Q, confirming that Q mutation mimics the effect of acetylation.

See also Figure S5.

observed with E113G and G178S mutants (Freudenthal et al., 2008). Overall, these results suggest that K20 acetylation triggers long-range structural changes impacting the distance between the protomers of the clamp.

DISCUSSION

Our results demonstrate that the sliding-clamp PCNA is acetylated in vivo to promote genome stability. We reveal that multiple acetylations occur on highly conserved lysines located at the sliding surface of the PCNA ring, an unlikely target surface for regulation of PCNA functions. Importantly, we demonstrate that PCNA is acetylated by Eco1 in response to DNA damage, a modification that stimulates sister-chromatid-mediated HR. Furthermore, we show that mimicking acetylation strongly suppresses the DNA damage sensitivity of cells carrying mutations in damage tolerance pathways. Finally, we report that acetylation of PCNA by Eco1 on lysine 20 induces long-range conformational changes, providing new insights into the mechanism of PCNA sliding on DNA to control the processivity of polymerases. Our findings suggest that the sliding of PCNA can be dynamically regulated at its inner surface, leading to conformational changes in the ring and the way it interacts with DNA. These results raise new questions and perspectives on the structural role of the ring and PCNA as a processivity factor.

Intricate Regulation at the Inner Surface of the PCNA Ring by Lysine Acetylation

It has been postulated that PCNA is required to stimulate DNA polymerases by increasing their processivity through its positive charges implicated in sliding on the DNA. This stimulation prevents polymerase dissociation from DNA synthesis, a model confirmed in vitro (Chilkova et al., 2007; Fukuda et al., 1995; Kochaniak et al., 2009; Laurence et al., 2008). This model intrigued us since it suggests that PCNA sliding is required only for polymerases to move along DNA but is not a direct means of

(G) PCNA acetylation stimulates intrachromosomal recombination between *leu2-112*::URA3::*leu2-k*. Cells were grown overnight with 0.001% MMS and plated to count recombination events and survival rates. Gene conversion represents cells growing on LEU+URA+ plates (gray), and overall recombination represents cells growing on LEU+ plates (white) events. Error bars are SEM of six independent experiments.

See also Figure S4.

Table 1. Crystallographic Data and Refinement Statistics for Acetylated PCNA

Data Collection	
Space group	$P2_12_12_1$
Cell dimensions: *a*, *b*, *c* (Å)	122.0, 122.3, 122.0
Cell dimensions: α, β, γ (°)	90.0, 90.0, 90.0
Resolution (Å)	86.3–3.27 (3.4–3.27)
R_{sym}	7.2 (64.2)
$I/\sigma I$	33.9 (2.5)
Completeness (%)	100.0 (96.7)
Redundancy	5.3 (6.3)
Refinement	
Resolution (Å)	49.8–3.27
No. reflections	28,983
R_{work}/R_{free}	21.3/23.1
No. protein atoms	5552
B-factors: protein (Å^2)	88.0
Molprobity score	1.73
RMSDs: bond lengths (Å)	0.005
RMSDs: bond angles (°)	1.03

Related to Figures 7 and S6. The dataset was collected on a single crystal. Highest resolution shell is shown in parenthesis. RMSDs, root-mean-square deviations.

regulation. This concept is even more puzzling since PCNA controls the activity of different classes of DNA polymerases (Sale, 2013). We decided to explore whether a regulatory mechanism to modulate the processivity of DNA polymerases and PCNA sliding exists. We found that multiple lysine residues located at the inner ring of the clamp and required for sliding are acetylated in response to DNA damage. In order to understand whether multiple acetylations have a biological significance in vivo, we generated different combinations of mutants with glutamine and arginine substitutions to respectively mimic either the acetylated or unacetylated residues while preventing acetylation on specific sites. Interestingly, we noted that these mutants exhibit a strong sensitivity to DNA damage, suppressed by reintroducing lysines, supporting an intricate regulation of this surface. This extensive mutational analysis provides unanticipated understanding of PCNA regulation since its internal surface was predicted to act solely as a line of positive charges. In addition, our data demonstrate that these lysines are in fact not interchangeable, illustrating how the sliding surface of PCNA is very complex, evolutionarily conserved, highly controlled, and critically important to promote genome stability. Importantly, our findings pave the way to an important change of perception about the PCNA ring, whose functions were thought to be regulated solely through its external surface (Mailand et al., 2013; Moldovan et al., 2007).

Acetylation of PCNA Stimulates HR and Suppresses the DNA Damage Sensitivity of Cells Lacking the Rad6/Rad18 Tolerance Pathway

Interestingly, we found that PCNA acetylation on K20 robustly suppresses the sensitivity to MMS of cells carrying mutations in the DNA damage tolerance pathway. Importantly, this suppression is not due to a slower S phase progression that would favor alternate repair pathways in front of the replication fork (Figures S7A and S7B). Furthermore, the capability of Pol30-K20Q/A substitutions to suppress the DNA damage sensitivity of TLS and template switching mutant cells revealed that only the K20Q acetylation mimic is effective for the K164R/*rad6*/*rad18* mutants. This functional link between Eco1-dependent acetylation of PCNA and the strong suppression of TLS mutants is consistent with the intriguing fact that *S. pombe* Eco1 is fused into a single protein with Polη, a merged protein containing both acetyltransferase (Tanaka et al., 2000) and lesion bypass activities (Madril et al., 2001). The suppression of the damage sensitivity of *rad5*/template switching mutant cells by both K20Q and K20A mutants is more likely due to an indirect effect, such as the absence of SUMOylation, not through PCNA acetylation per se. It will be of interest to decipher the intriguing link among SUMO, Eco1, and PCNA acetylation (Moldovan et al., 2006). We propose that Eco1-dependent acetylation of PCNA could function at a lesion by favoring Polδ removal from DNA, specifically upon encountering DNA lesions, resulting in the stimulation of sister-chromatid recombination (Figure S7C). An interesting observation is that the sequence surrounding PCNA K20 shows similarity to an Eco1-dependent acetylation site on cohesin subunit Smc3 (Figure S3I) (Unal et al., 2008). Altogether, acetylation of PCNA by Eco1 could cooperate with acetylation of cohesins to change the speed of replication forks at genome impediments (Terret et al., 2009), ultimately stimulating recombination between sister chromatids.

Long-Distance Structural Changes Observed in the PCNA-K20ac Ring

Since acetylation occurs at the sliding surface and affects the processivity of polymerase δ, it was important to determine its impact on the structure of the PCNA ring. Our findings that acetylation correlates with some long-range conformational changes is striking since other highly studied PTMs of PCNA do not alter its structure (Freudenthal et al., 2010, 2011). In contrast, these modifications adopt distinct modes of association to PCNA in order to increase the possible surfaces of recruitment of effectors (Tsutakawa et al., 2015). The concept that the conformational change linked to PCNA acetylation could suppress the DNA damage sensitivity of mutants in TLS is consistent with reported observations with PCNA E113G and G178S mutants at the interface of the protomers (β sheets 9 and 13; note Y114 slightly closer to D150 in PCNA-K20ac; Figures 7C and S6C). These mutants also produce conformational changes at the interface between protomers and are defective in TLS (Dieckman and Washington, 2013; Freudenthal et al., 2008). Interestingly, while these mutants inhibit the DNA damage tolerance pathway (Zhang et al., 2006), they are not reported to stimulate HR. Therefore, the impact of Eco1-dependent acetylation of PCNA may play out at different levels. A mobile acetylated lysine residue inside the ring could affect sliding when encountering DNA lesions, transiently favoring the removal of Polδ from DNA synthesis in combination with long-distance conformational changes. The structural impact at the interface of protomers could also disfavor TLS, as reported for E113G and G178S mutants. The

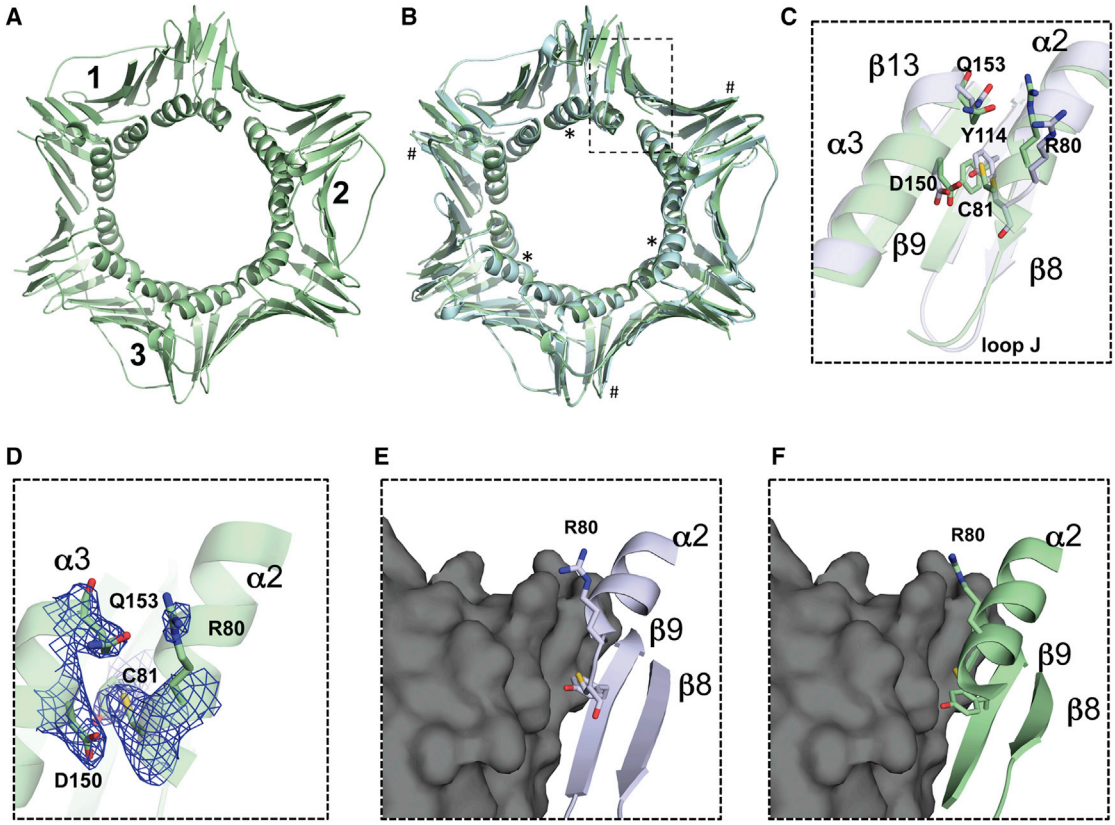

Figure 7. Acetylation of K20 on PCNA Correlates with Long-Range Structural Changes Impacting the Interface between Protomers

(A) Cartoon representation of PCNA-K20ac, highlighted in green, in which the three protomers are indicated.

(B) Cartoon representation of an alignment between acetylated (green) and unacetylated PCNA (light blue). The * and the # denote the position of K20 and K164 in the structure, respectively.

(C) Zoomed view of the interface between two protomers illustrating the structural differences between the acetylated (green) and the unacetylated (light blue) forms of PCNA. Residues undergoing noticeable structural changes are also highlighted in stick, and relevant secondary structures are labeled. Oxygen and nitrogen atoms are rendered in red and blue, respectively.

(D) Shown is the omit map for residues at the interface between α3 of one protomer and α2 of another protomer. The map is contoured at 1.5σ. Key residues are indicated as in (C).

(E and F) Zoomed view on the interface between the surface on one protomer and the indicated secondary structures of the neighboring protomer of the unacetylated (E) and acetylated (F) PCNA. Key residues are shown as in (C).

See also Figure S6.

mechanism for stimulation of HR is less clear to envision from the structural viewpoint. The loss of SUMOylation does not seem to be due to a large change in the structure of the loop carrying the K164 residue (Figures 7B and S6D). On the other hand, recent reports strengthen the importance of the interface between PCNA subunits for TLS and HR (Halmai et al., 2016; Streich and Lima, 2016). Strikingly, Ubc9, the E2 of the SUMO ligase Siz1, was shown to bind at the interface between protomers to allow SUMOylation of PCNA, in the same region where we observe structural changes in PCNA-K20ac (Streich and Lima, 2016). This may play a role in the fact that our PCNA K20 mutants are not SUMOylated in vivo (Figure 5D).

In addition to structural changes, the neutralization of the positive charges induced by PCNA acetylation certainly affects its interactions with the DNA phosphate backbone during sliding transactions. Indeed, while K20 normally interacts with the side chain of D17 in PCNA structure (Krishna et al., 1994), we observed that K20Ac is mobile, which could directly impact interaction with the phosphate backbone. This is supported by the observation that subtle structural alterations in the α helices or at the subunit interface cause repair defects (Dieckman et al., 2013). Importantly, it was observed that PCNA α helices are dynamic (De Biasio et al., 2011) and also alternate to be more stable (Fang et al., 2014), both states proposed to be functionally linked with DNA interaction. For all these reasons, it will be interesting to determine the structural effect of multiple acetylations required to promote DNA damage resistance (Figure 2). The exact molecular dynamic of the interactions between DNA and the sliding surface is unknown. Future challenges will be to address the structure and the motion of PCNA on DNA during sliding transactions. These experiments will reveal how acetylation of PCNA affects its sliding and the accommodation of the polymerases. This may be linked to the concept that PCNA by itself diffuses along DNA with two different modes (Kochaniak et al., 2009).

Although further studies are needed to clarify these points, our findings uncovered a new critical mechanism of response to stalled forks and control of PCNA sliding on the DNA.

EXPERIMENTAL PROCEDURES

Yeast Strains, Plasmids, Mutagenesis, Growth, and Drug Sensitivity Assays

Yeast manipulations, culture, and transformations were performed according to standard protocols. See Supplemental Experimental Procedures and Tables S2 and S3 for full details.

Protein Purifications, PCNA Modifications, and Crystal Structure

DNA polymerases, RPA, and RFC were prepared as described previously (Li et al., 2013). PCNA mutants and NuA4 complex (Epl1-Flag) were purified from yeast through the Flag epitope following standard procedures. Eco1 and RTT109-Vps75 were purified from bacteria. Recombinant PCNA acetylated at single sites was obtained with the protocol described in Neumann et al. (2009). See Supplemental Experimental Procedures for full details. Crystallization and crystal structure determination of acetylated PCNA were performed following standard procedures and are described in detail in the Supplemental Experimental Procedures. This crystal structure has been deposited to the protein databank (PDB: 5T9D).

In Vitro Acetyltransferase and DNA Polymerase Assays

Acetyltransferase assays with 500 ng purified PCNA were performed following standard conditions for detection of histone acetylation. Details of DNA polymerase assays, the in vitro reconstituted system, and reactions were described previously (Li et al., 2013). See Supplemental Experimental Procedures for full details.

Analysis of Recombination Rate

Intrachromosomal recombination was measured using a strain carrying the *leu2-112*::URA3::*leu2-k* cassette. Exponential growing cells were treated with 0.001% MMS and incubated overnight at 30°C. Cells were washed in 2.5% sodium thiosulfate to inactivate MMS. Cells were diluted and plated to determine viability, overall recombination (Leu+), and gene conversion (Leu+, Ura+) rates. Recombination rates were calculated as a frequency of survival cells.

SUPPLEMENTAL INFORMATION

Supplemental Information includes Supplemental Experimental Procedures, seven figures, and three tables and can be found with this article online at http://dx.doi.org/10.1016/j.molcel.2016.10.033.

AUTHOR CONTRIBUTIONS

The project was conceived and designed by P.B., A.V., T.S., and J.C.; experiments were carried out by P.B., J.L., J.-P.L., Y.C., V.T., and J.S.B.; A.-C.G. supervised J.-P.L.; J.-F.C. analyzed the structural data; and P.B. and J.C. wrote the paper.

ACKNOWLEDGMENTS

We thank members of the J.C. lab, Alberto Ciccia, and Damien D'Amours for comments on the manuscript. We are grateful to Helle Ulrich for the anti-Pol30 antibody and advice, to Jason Chin for the system to purify acetylated recombinant PCNA, and to Stefan Jentsch and Jennifer Gerton for sharing plasmids and strains. This work was supported by grants from the Canadian Institutes of Health Research (CIHR) to A.-C.G. (MOP-123322), J.-F.C. (MOP-136816), and J.C. (MOP-14308; FDN-143314). J.-P.L. was supported by CIHR and TD Bank Health Research Fellowships. A.-C.G. holds the Lea Reichmann Chair in Cancer Proteomics. A.-C.G., J.-F.C., and J.C. hold the Canada Research Chairs in Functional Proteomics, Structural Biology and Epigenetics, and Chromatin Biology and Molecular Epigenetics, respectively.

Received: July 18, 2016
Revised: October 9, 2016
Accepted: October 24, 2016
Published: December 1, 2016

REFERENCES

Branzei, D., and Foiani, M. (2010). Maintaining genome stability at the replication fork. Nat. Rev. Mol. Cell Biol. *11*, 208–219.

Cazzalini, O., Sommatis, S., Tillhon, M., Dutto, I., Bachi, A., Rapp, A., Nardo, T., Scovassi, A.I., Necchi, D., Cardoso, M.C., et al. (2014). CBP and p300 acetylate PCNA to link its degradation with nucleotide excision repair synthesis. Nucleic Acids Res. *42*, 8433–8448.

Chen, Y., Zhao, W., Yang, J.S., Cheng, Z., Luo, H., Lu, Z., Tan, M., Gu, W., and Zhao, Y. (2012). Quantitative acetylome analysis reveals the roles of SIRT1 in regulating diverse substrates and cellular pathways. Mol. Cell. Proteomics *11*, 1048–1062.

Chilkova, O., Stenlund, P., Isoz, I., Stith, C.M., Grabowski, P., Lundström, E.B., Burgers, P.M., and Johansson, E. (2007). The eukaryotic leading and lagging strand DNA polymerases are loaded onto primer-ends via separate mechanisms but have comparable processivity in the presence of PCNA. Nucleic Acids Res. *35*, 6588–6597.

Choudhary, C., Kumar, C., Gnad, F., Nielsen, M.L., Rehman, M., Walther, T.C., Olsen, J.V., and Mann, M. (2009). Lysine acetylation targets protein complexes and co-regulates major cellular functions. Science *325*, 834–840.

Ciccia, A., and Elledge, S.J. (2010). The DNA damage response: making it safe to play with knives. Mol. Cell *40*, 179–204.

Collins, S.R., Miller, K.M., Maas, N.L., Roguev, A., Fillingham, J., Chu, C.S., Schuldiner, M., Gebbia, M., Recht, J., Shales, M., et al. (2007). Functional dissection of protein complexes involved in yeast chromosome biology using a genetic interaction map. Nature *446*, 806–810.

De Biasio, A., Sánchez, R., Prieto, J., Villate, M., Campos-Olivas, R., and Blanco, F.J. (2011). Reduced stability and increased dynamics in the human proliferating cell nuclear antigen (PCNA) relative to the yeast homolog. PLoS ONE *6*, e16600.

Dieckman, L.M., and Washington, M.T. (2013). PCNA trimer instability inhibits translesion synthesis by DNA polymerase η and by DNA polymerase δ. DNA Repair (Amst.) *12*, 367–376.

Dieckman, L.M., Freudenthal, B.D., and Washington, M.T. (2012). PCNA structure and function: insights from structures of PCNA complexes and post-translationally modified PCNA. Subcell. Biochem. *62*, 281–299.

Dieckman, L.M., Boehm, E.M., Hingorani, M.M., and Washington, M.T. (2013). Distinct structural alterations in proliferating cell nuclear antigen block DNA mismatch repair. Biochemistry *52*, 5611–5619.

Fang, J., Nevin, P., Kairys, V., Venclovas, C., Engen, J.R., and Beuning, P.J. (2014). Conformational analysis of processivity clamps in solution demonstrates that tertiary structure does not correlate with protein dynamics. Structure *22*, 572–581.

Freudenthal, B.D., Ramaswamy, S., Hingorani, M.M., and Washington, M.T. (2008). Structure of a mutant form of proliferating cell nuclear antigen that blocks translesion DNA synthesis. Biochemistry *47*, 13354–13361.

Freudenthal, B.D., Gakhar, L., Ramaswamy, S., and Washington, M.T. (2010). Structure of monoubiquitinated PCNA and implications for translesion synthesis and DNA polymerase exchange. Nat. Struct. Mol. Biol. *17*, 479–484.

Freudenthal, B.D., Brogie, J.E., Gakhar, L., Kondratick, C.M., and Washington, M.T. (2011). Crystal structure of SUMO-modified proliferating cell nuclear antigen. J. Mol. Biol. *406*, 9–17.

Fukuda, K., Morioka, H., Imajou, S., Ikeda, S., Ohtsuka, E., and Tsurimoto, T. (1995). Structure-function relationship of the eukaryotic DNA replication factor, proliferating cell nuclear antigen. J. Biol. Chem. *270*, 22527–22534.

Georgescu, R.E., Kim, S.S., Yurieva, O., Kuriyan, J., Kong, X.P., and O'Donnell, M. (2008). Structure of a sliding clamp on DNA. Cell *132*, 43–54.

Gordillo, M., Vega, H., Trainer, A.H., Hou, F., Sakai, N., Luque, R., Kayserili, H., Basaran, S., Skovby, F., Hennekam, R.C., et al. (2008). The molecular mechanism underlying Roberts syndrome involves loss of ESCO2 acetyltransferase activity. Hum. Mol. Genet. *17*, 2172–2180.

Halmai, M., Frittmann, O., Szabo, Z., Daraba, A., Gali, V.K., Balint, E., and Unk, I. (2016). Mutations at the subunit interface of yeast proliferating cell nuclear antigen reveal a versatile regulatory domain. PLoS ONE *11*, e0161307.

Henriksen, P., Wagner, S.A., Weinert, B.T., Sharma, S., Bacinskaja, G., Rehman, M., Juffer, A.H., Walther, T.C., Lisby, M., and Choudhary, C. (2012). Proteome-wide analysis of lysine acetylation suggests its broad regulatory scope in Saccharomyces cerevisiae. Mol. Cell. Proteomics *11*, 1510–1522.

Hoege, C., Pfander, B., Moldovan, G.L., Pyrowolakis, G., and Jentsch, S. (2002). RAD6-dependent DNA repair is linked to modification of PCNA by ubiquitin and SUMO. Nature *419*, 135–141.

Ivanov, I., Chapados, B.R., McCammon, J.A., and Tainer, J.A. (2006). Proliferating cell nuclear antigen loaded onto double-stranded DNA: dynamics, minor groove interactions and functional implications. Nucleic Acids Res. *34*, 6023–6033.

Johansson, E., Garg, P., and Burgers, P.M. (2004). The Pol32 subunit of DNA polymerase delta contains separable domains for processive replication and proliferating cell nuclear antigen (PCNA) binding. J. Biol. Chem. *279*, 1907–1915.

Kelman, Z., and O'Donnell, M. (1995). Structural and functional similarities of prokaryotic and eukaryotic DNA polymerase sliding clamps. Nucleic Acids Res. *23*, 3613–3620.

Kochaniak, A.B., Habuchi, S., Loparo, J.J., Chang, D.J., Cimprich, K.A., Walter, J.C., and van Oijen, A.M. (2009). Proliferating cell nuclear antigen uses two distinct modes to move along DNA. J. Biol. Chem. *284*, 17700–17710.

Krishna, T.S., Kong, X.P., Gary, S., Burgers, P.M., and Kuriyan, J. (1994). Crystal structure of the eukaryotic DNA polymerase processivity factor PCNA. Cell *79*, 1233–1243.

Laurence, T.A., Kwon, Y., Johnson, A., Hollars, C.W., O'Donnell, M., Camarero, J.A., and Barsky, D. (2008). Motion of a DNA sliding clamp observed by single molecule fluorescence spectroscopy. J. Biol. Chem. *283*, 22895–22906.

Lengronne, A., McIntyre, J., Katou, Y., Kanoh, Y., Hopfner, K.P., Shirahige, K., and Uhlmann, F. (2006). Establishment of sister chromatid cohesion at the S. cerevisiae replication fork. Mol. Cell *23*, 787–799.

Li, J., Holzschu, D.L., and Sugiyama, T. (2013). PCNA is efficiently loaded on the DNA recombination intermediate to modulate polymerase δ, η, and ζ activities. Proc. Natl. Acad. Sci. USA *110*, 7672–7677.

Lu, S., Goering, M., Gard, S., Xiong, B., McNairn, A.J., Jaspersen, S.L., and Gerton, J.L. (2010). Eco1 is important for DNA damage repair in S. cerevisiae. Cell Cycle *9*, 3315–3327.

Lundby, A., Lage, K., Weinert, B.T., Bekker-Jensen, D.B., Secher, A., Skovgaard, T., Kelstrup, C.D., Dmytriyev, A., Choudhary, C., Lundby, C., and Olsen, J.V. (2012). Proteomic analysis of lysine acetylation sites in rat tissues reveals organ specificity and subcellular patterns. Cell Rep. *2*, 419–431.

Madril, A.C., Johnson, R.E., Washington, M.T., Prakash, L., and Prakash, S. (2001). Fidelity and damage bypass ability of Schizosaccharomyces pombe Eso1 protein, comprised of DNA polymerase eta and sister chromatid cohesion protein Ctf7. J. Biol. Chem. *276*, 42857–42862.

Mailand, N., Gibbs-Seymour, I., and Bekker-Jensen, S. (2013). Regulation of PCNA-protein interactions for genome stability. Nat. Rev. Mol. Cell Biol. *14*, 269–282.

McNally, R., Bowman, G.D., Goedken, E.R., O'Donnell, M., and Kuriyan, J. (2010). Analysis of the role of PCNA-DNA contacts during clamp loading. BMC Struct. Biol. *10*, 3.

Moldovan, G.L., Pfander, B., and Jentsch, S. (2006). PCNA controls establishment of sister chromatid cohesion during S phase. Mol. Cell *23*, 723–732.

Moldovan, G.L., Pfander, B., and Jentsch, S. (2007). PCNA, the maestro of the replication fork. Cell *129*, 665–679.

Naryzhny, S.N., and Lee, H. (2004). The post-translational modifications of proliferating cell nuclear antigen: acetylation, not phosphorylation, plays an important role in the regulation of its function. J. Biol. Chem. *279*, 20194–20199.

Neumann, H., Hancock, S.M., Buning, R., Routh, A., Chapman, L., Somers, J., Owen-Hughes, T., van Noort, J., Rhodes, D., and Chin, J.W. (2009). A method for genetically installing site-specific acetylation in recombinant histones defines the effects of H3 K56 acetylation. Mol. Cell *36*, 153–163.

Papouli, E., Chen, S., Davies, A.A., Huttner, D., Krejci, L., Sung, P., and Ulrich, H.D. (2005). Crosstalk between SUMO and ubiquitin on PCNA is mediated by recruitment of the helicase Srs2p. Mol. Cell *19*, 123–133.

Pfander, B., Moldovan, G.L., Sacher, M., Hoege, C., and Jentsch, S. (2005). SUMO-modified PCNA recruits Srs2 to prevent recombination during S phase. Nature *436*, 428–433.

Renaud-Young, M., Lloyd, D.C., Chatfield-Reed, K., George, I., Chua, G., and Cobb, J. (2015). The NuA4 complex promotes translesion synthesis (TLS)-mediated DNA damage tolerance. Genetics *199*, 1065–1076.

Rolef Ben-Shahar, T., Heeger, S., Lehane, C., East, P., Flynn, H., Skehel, M., and Uhlmann, F. (2008). Eco1-dependent cohesin acetylation during establishment of sister chromatid cohesion. Science *321*, 563–566.

Sale, J.E. (2013). Translesion DNA synthesis and mutagenesis in eukaryotes. Cold Spring Harb. Perspect. Biol. *5*, a012708.

Sjögren, C., and Ström, L. (2010). S-phase and DNA damage activated establishment of sister chromatid cohesion—importance for DNA repair. Exp. Cell Res. *316*, 1445–1453.

Stelter, P., and Ulrich, H.D. (2003). Control of spontaneous and damage-induced mutagenesis by SUMO and ubiquitin conjugation. Nature *425*, 188–191.

Streich, F.C., Jr., and Lima, C.D. (2016). Capturing a substrate in an activated RING E3/E2-SUMO complex. Nature *536*, 304–308.

Tanaka, K., Yonekawa, T., Kawasaki, Y., Kai, M., Furuya, K., Iwasaki, M., Murakami, H., Yanagida, M., and Okayama, H. (2000). Fission yeast Eso1p is required for establishing sister chromatid cohesion during S phase. Mol. Cell. Biol. *20*, 3459–3469.

Terret, M.E., Sherwood, R., Rahman, S., Qin, J., and Jallepalli, P.V. (2009). Cohesin acetylation speeds the replication fork. Nature *462*, 231–234.

Tsutakawa, S.E., Yan, C., Xu, X., Weinacht, C.P., Freudenthal, B.D., Yang, K., Zhuang, Z., Washington, M.T., Tainer, J.A., and Ivanov, I. (2015). Structurally distinct ubiquitin- and sumo-modified PCNA: implications for their distinct roles in the DNA damage response. Structure *23*, 724–733.

Unal, E., Heidinger-Pauli, J.M., Kim, W., Guacci, V., Onn, I., Gygi, S.P., and Koshland, D.E. (2008). A molecular determinant for the establishment of sister chromatid cohesion. Science *321*, 566–569.

Yu, Y., Cai, J.P., Tu, B., Wu, L., Zhao, Y., Liu, X., Li, L., McNutt, M.A., Feng, J., He, Q., et al. (2009). Proliferating cell nuclear antigen is protected from degradation by forming a complex with MutT Homolog2. J. Biol. Chem. *284*, 19310–19320.

Zeman, M.K., and Cimprich, K.A. (2014). Causes and consequences of replication stress. Nat. Cell Biol. *16*, 2–9.

Zhang, H., Gibbs, P.E., and Lawrence, C.W. (2006). The Saccharomyces cerevisiae rev6-1 mutation, which inhibits both the lesion bypass and the recombination mode of DNA damage tolerance, is an allele of POL30, encoding proliferating cell nuclear antigen. Genetics *173*, 1983–1989.

Molecular Cell, Volume *65*

Supplemental Information

Acetylation of PCNA Sliding Surface by Eco1 Promotes Genome Stability through Homologous Recombination

Pierre Billon, Jian Li, Jean-Philippe Lambert, Yizhang Chen, Véronique Tremblay, Joseph S. Brunzelle, Anne-Claude Gingras, Alain Verreault, Tomohiko Sugiyama, Jean-Francois Couture, and Jacques Côté

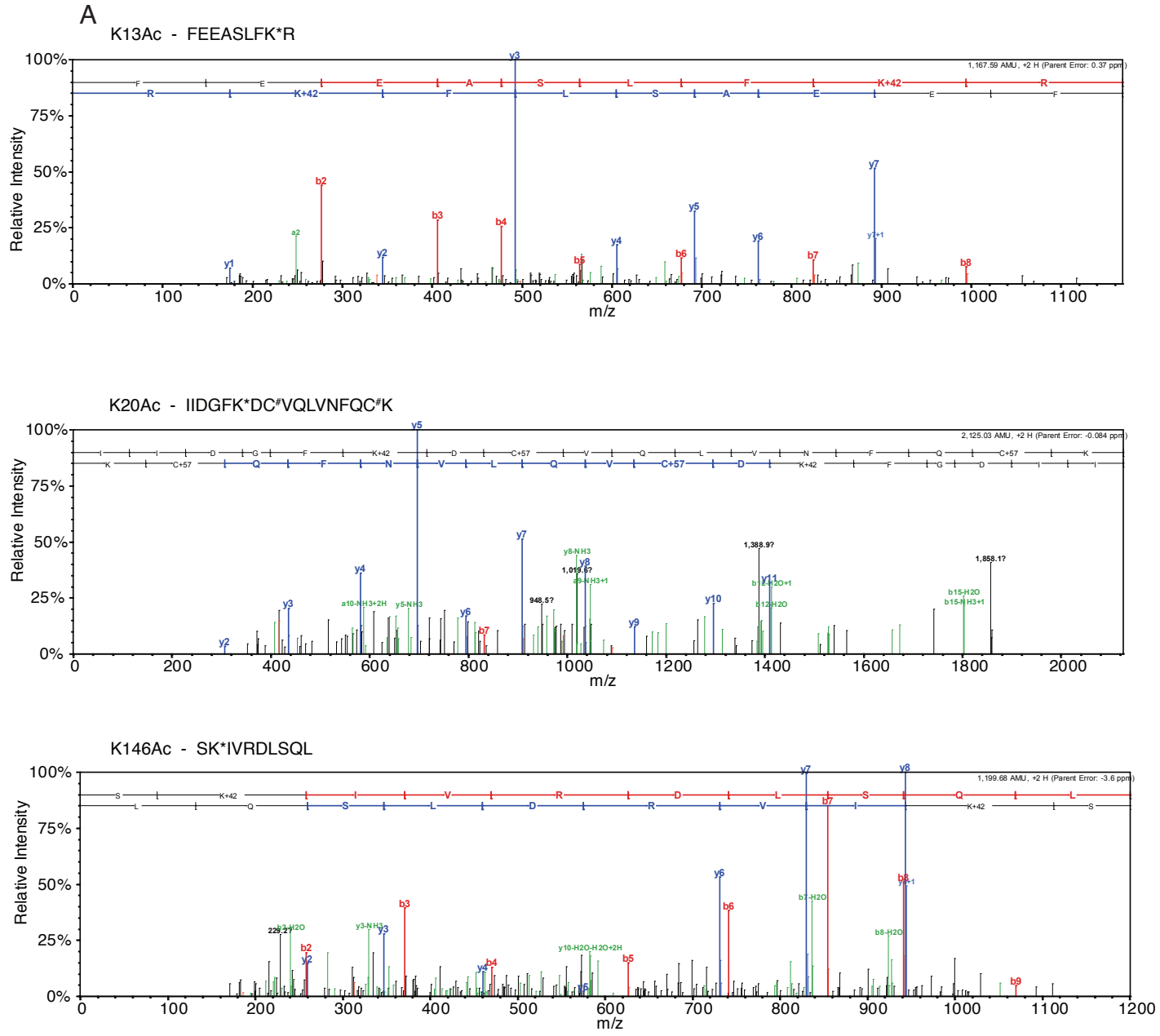

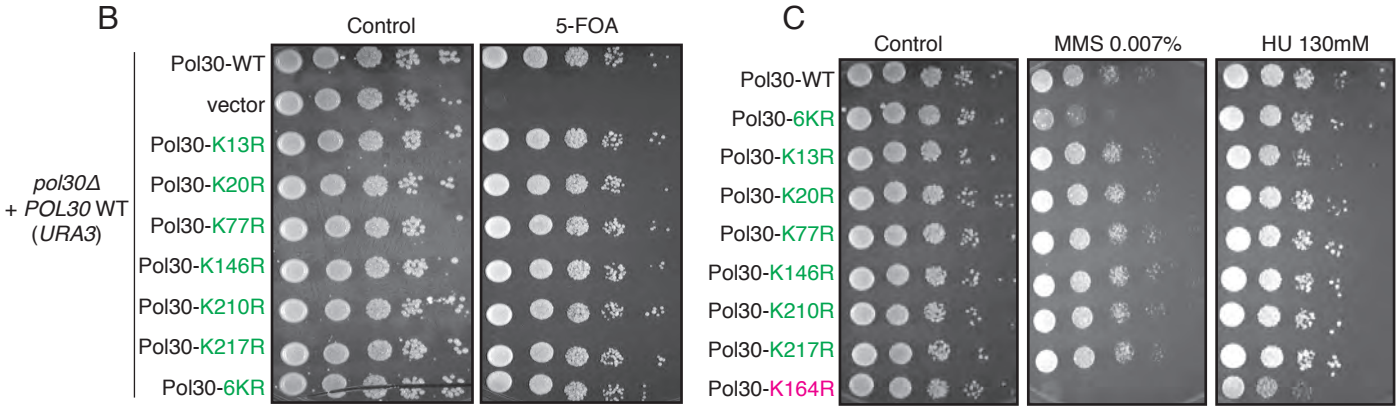

Billon et al. Supplemental Fig. S1

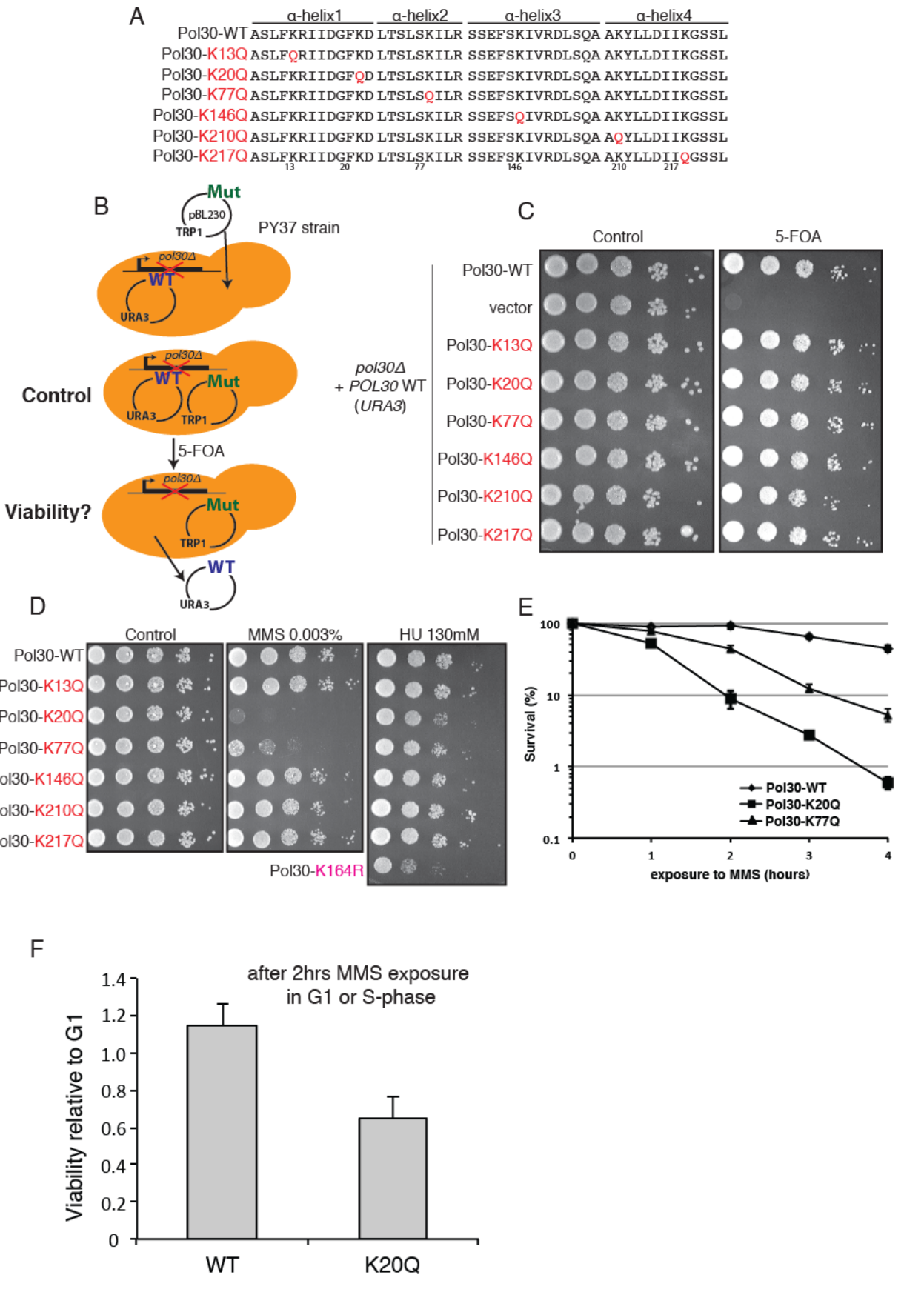

Billon et al. Supplemental Fig. S2

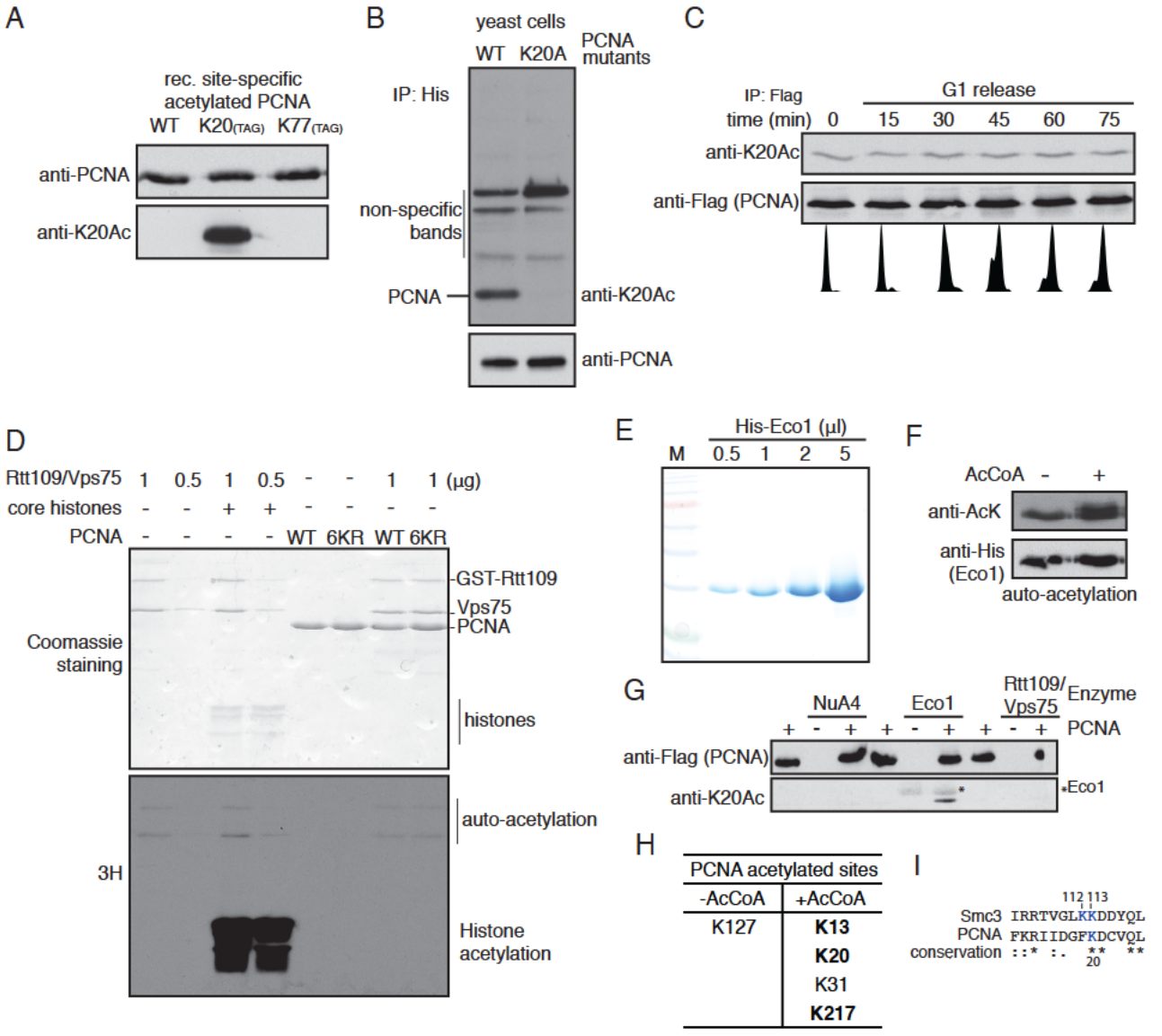

Billon et al. Supplemental Fig. S3

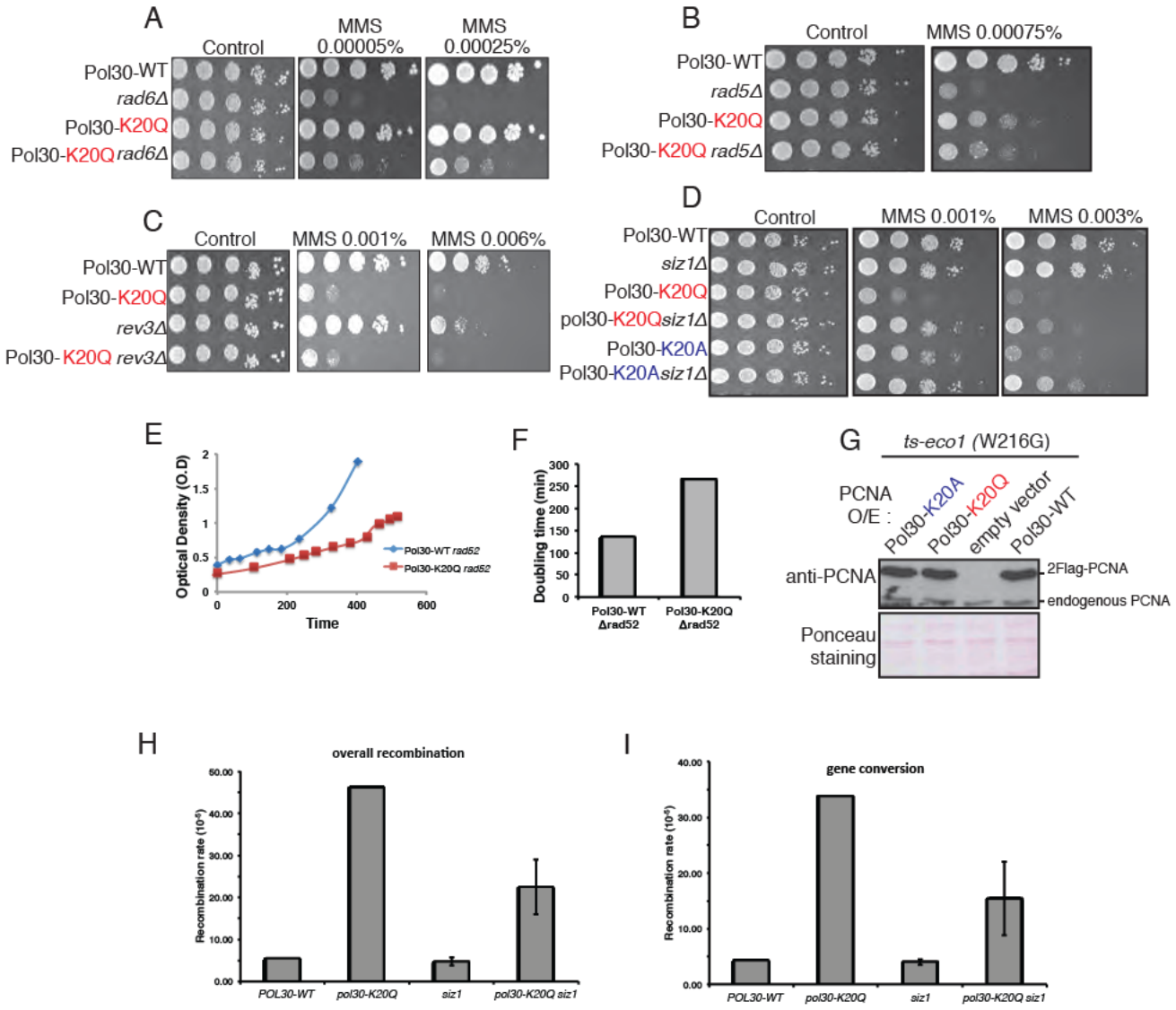

Billon et al. Supplemental Fig. S4

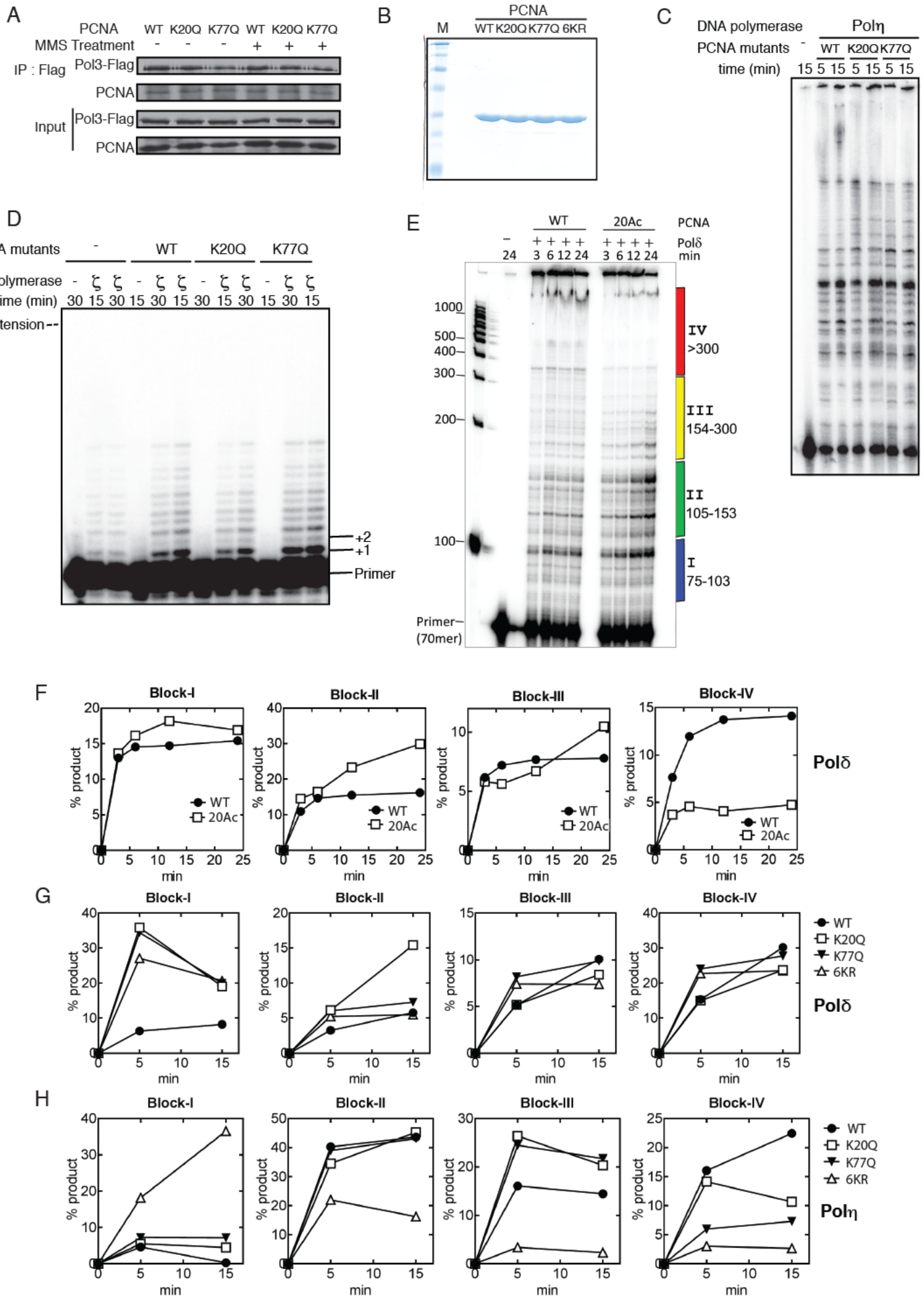

Billon et al. Supplemental Fig. S5

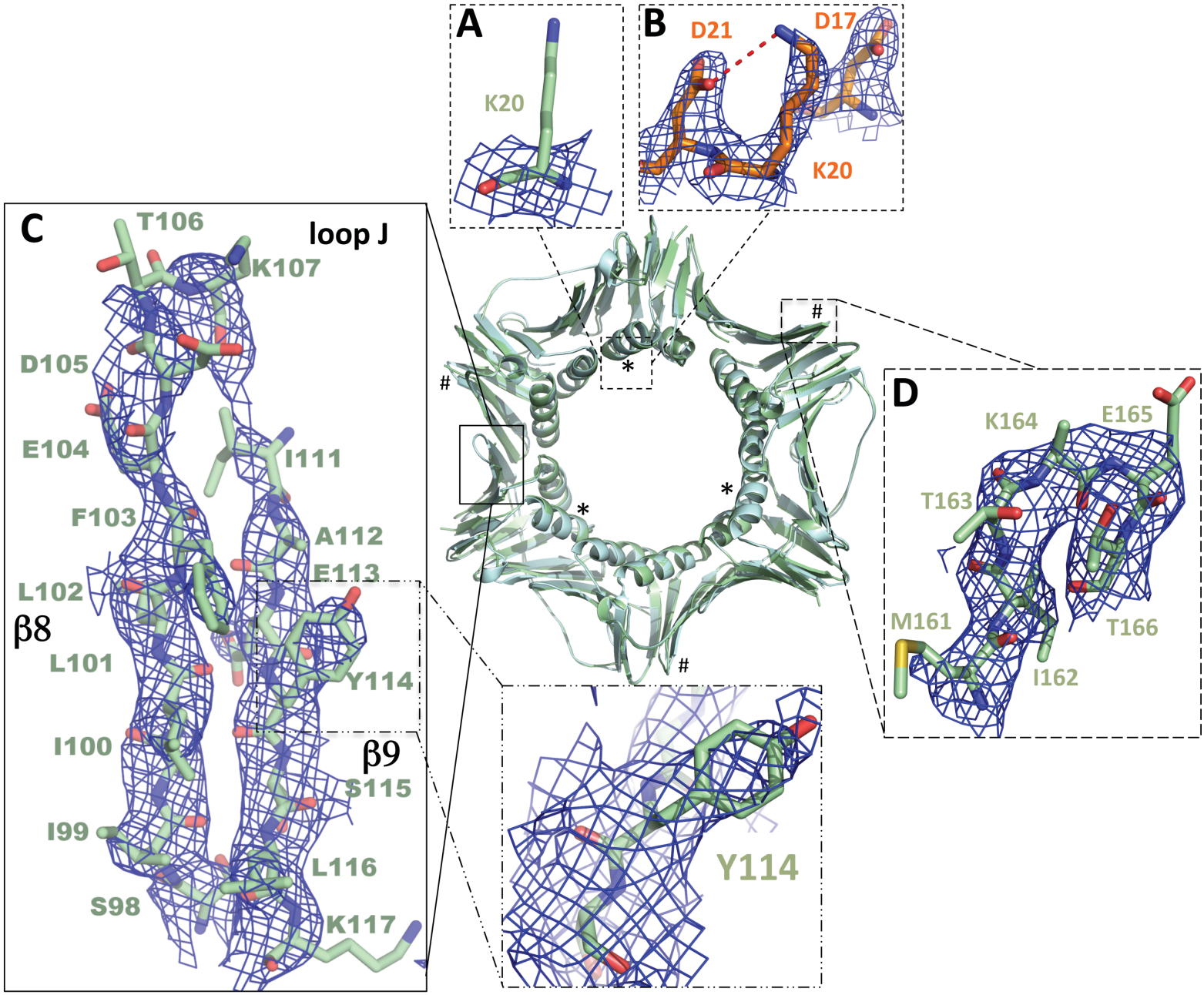

Billon et al. Supplemental Fig. S6

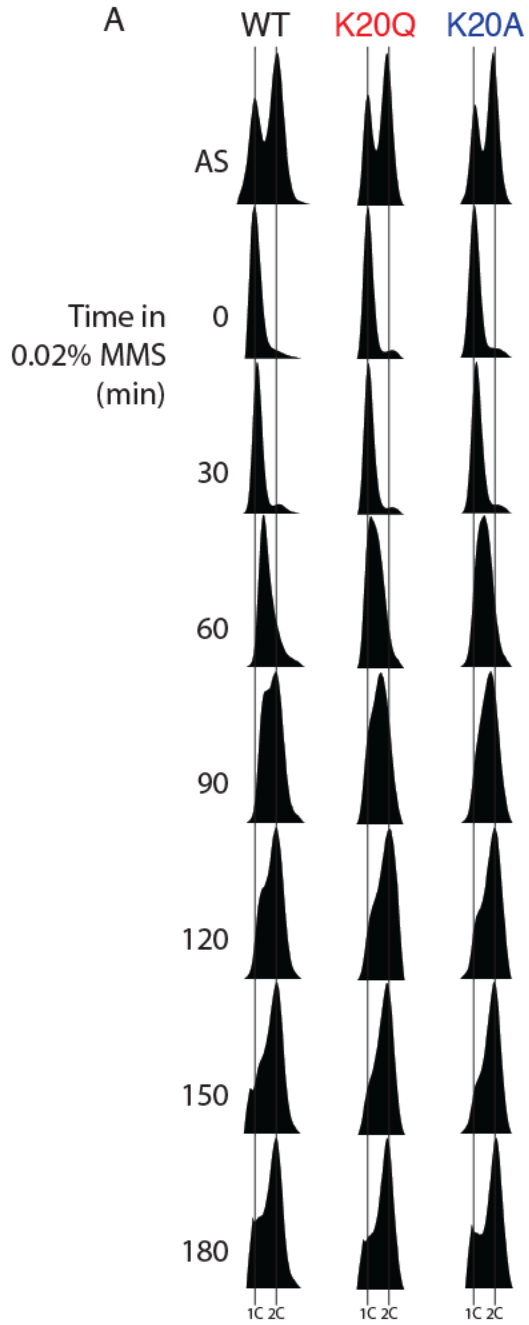

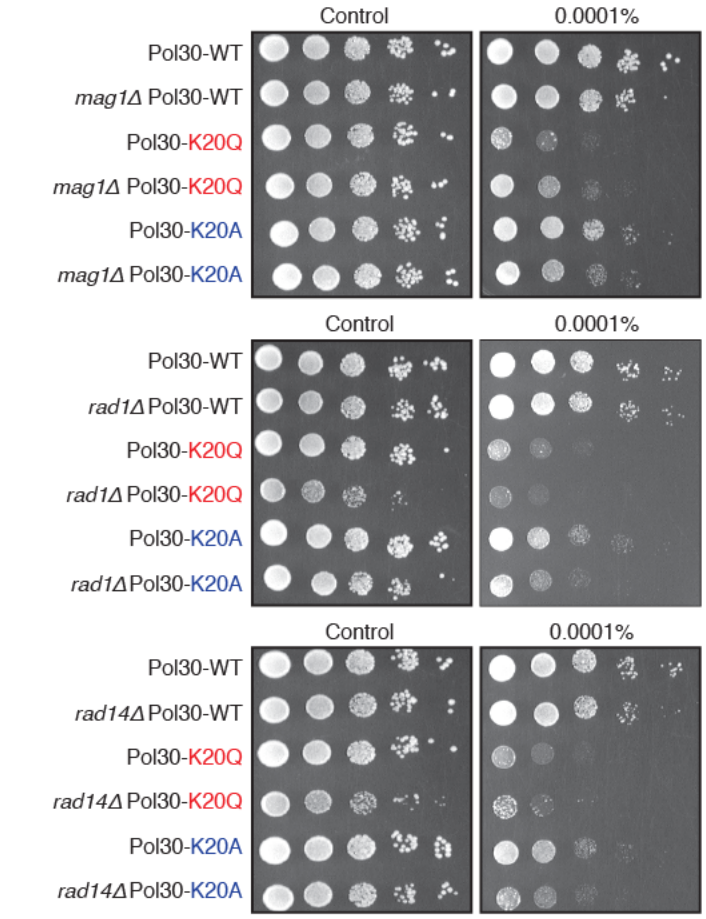

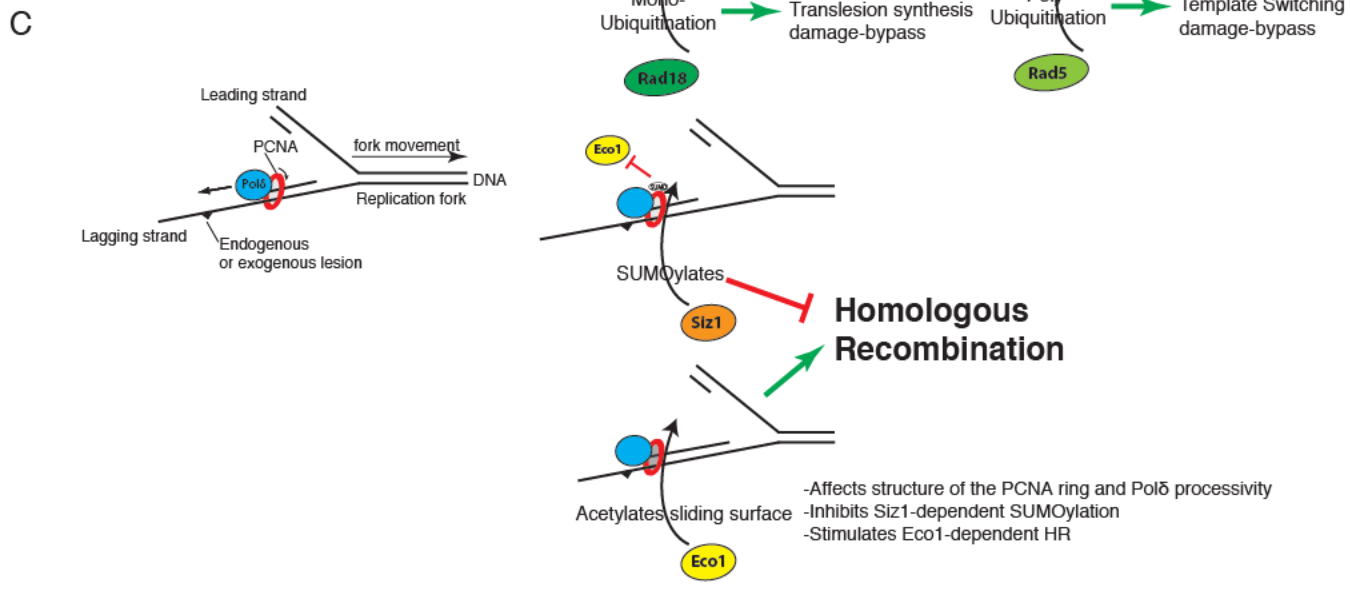

Billon et al. Supplemental Fig. S7

SUPPLEMENTAL FIGURE AND TABLE LEGENDS

Supplemental Figure S1. Identification of acetylated residues on PCNA by tandem mass spectrometry, viability and sensitivity to MMS and HU of cells expressing PCNA with single lysine to arginine substitutions, related to Figures 1 and 2.
(A) Flag-tagged PCNA was purified from exponentially growing cells treated with 0.05% MMS for 2 hours at 30°C. MS/MS analysis of tryptic peptides was performed and MS/MS spectrum of 3 acetylated peptides are shown with major b- and y-ions labeled. **(B)** Dilution spot assay of *pol30*Δ cells expressing *POL30*-WT (*URA3* plasmid) and complemented with the indicated mutants (*TRP1* plasmid). Viability is evaluated by growth on 5-FOA compared to control plate. **(C)** Sensitivity to MMS and HU of the indicated mutants. The *pol30-K164R* mutant is used as a control for drug sensitivity.

Supplemental Figure S2. Viability and MMS/HU sensitivity of cells expressing PCNA lysine to glutamine substitution mutants, related to Figure 2.
(A) Sequence alignment of the 4 α-helices for each single lysine to glutamine mutants used in Figure 2A. **(B)** Schematic representation of the plasmid shuffling method used to verify the viability of each mutant in the PY37 strain. **(C)** Viability of the single acetyl-mimic mutants in presence and absence of 5-FOA. **(D)** Growth of the *pol30* mutants at indicated concentration of HU or MMS. **(E)** Survival curve of cells expressing *pol30-K20Q* and *pol30-K77Q* mutants during exposure to 0.2% MMS. Error-bars indicate s.e.m of three independent experiments. **(F)** G1 synchronized cells were treated with 0.03% MMS for 2 hours or released in S phase with 0.03% MMS. After treatment, survival rate was determined by plating about 100 survival cells/plates. Error-bars are s.e.m of 6 independent experiments.

Supplemental Figure S3. Validation of the K20ac antibody, specific detection of PCNA acetylated on K20, its cell cycle regulation and tested acetyltransferase activities, related to Figure 3.
(A) Validation and specificity of the anti-K20ac antibody on WT recombinant PCNA or acetylated at single sites K20 or K77. Anti-PCNA is used as loading control. **(B)** Validation and specificity of the anti-K20Ac antibody on PCNA purified from yeast cells. His-tagged Pol30-WT and Pol30-K20A mutant were purified under denaturing condition from whole cell extract using Ni-NTA resin, followed by a western blot with the antibody raised against the K20Ac site on PCNA. The antibody shows clear specific signal on PCNA from yeast cells, as none is detected with the K20A mutant. Total PCNA signal (anti-PCNA) is used as loading control. **(C)** Monitoring of the cell cycle regulation of K20ac. **(D)** *In vitro* acetyltransferase assay on histones and recombinant PCNA using purified Rtt109/Vps75 enzyme and radioactive acetyl-CoA (AcCoA). Reactions were loaded on gel, followed by coomassie staining and fluorography. **(E)** Coomassie stained gel showing the purification of recombinant Eco1. **(F)** *In vitro* auto-acetylation of recombinant Eco1 as detected by western blot with an anti-acetyl lysine antibody, as control for activity. **(G)** *In vitro* acetylation assay of PCNA using purified NuA4, Rtt109/Vps75 and Eco1 acetyltransferases shows specific acetylation of K20 by Eco1. Western blot analysis of the indicated acetylation assays using anti-K20Ac antibody. (*) non-specific band due to recombinant Eco1 itself. **(H)** Acetylated lysines mapped on

PCNA after *in vitro* acetylation by Eco1, detected by mass spectrometry. Lysines at the inner surface of the ring are in bold. **(I)** Alignment of amino acid sequences surrounding Pol30-K20 and Smc3-K112,K113 using Clustal W. (*) identical residue, (:) similar residue, (.) weakly similar residue.

Supplemental Figure S4. Genetic interactions between *pol30-K20Q* and postreplication repair genes, related to Figures 5 and 6.
Genetic interactions between the *pol30-K20Q* allele and *rad6* **(A)**, *rad5* **(B)** and *rev3* **(C)** reveal suppression of DNA damage tolerance pathways. MMS sensitivity of *rad6*, *rad5* and *rev3 rad5* mutant cells is suppressed by expression of the PCNA K20Q mutant, while loss of *REV3* does not alter sensitivity of *pol30-K20Q* cells. **(D)** Deletion of *SIZ1* partially suppresses MMS sensitivity of *pol30-K20Q* and *pol30-K20A* mutant cells. Growth curve **(E)** and doubling time **(F)** of *rad52* cells expressing normal PCNA or the *pol30-K20Q* allele, showing clear growth defect in normal media. **(G)** anti-PCNA western blot on whole cell extracts showing Flag-PCNA overexpression (O/E; wild type or K20Q mutant) over endogenous PCNA in the *eco1-W216G* ts strain. Ponceau staining of the membrane is shown as loading control. **(H-I)** PCNA acetylation mimic stimulates homologous recombination even in the absence of Siz1/SUMO-PCNA. *pol30-K20Q* stimulates intrachromosomal recombination between *leu2-112*::URA3::*leu2-k*, even in a *siz1* mutant background. Cells were grown overnight with 0.001% MMS and plated to count recombination events and survival rates. Overall recombination (H) represents cells growing on LEU+ plates (white) and gene conversion (I) represents cells growing on LEU+URA+ plates (grey). Error bars are s.e.m of 3 independent clones. *POL30-WT* and *pol30-K20Q* are single clones used as control.

Supplemental Figure S5. *In vitro* DNA synthesis using PCNA mutants and interaction with DNA polymerase *in vivo*, related to Figure 6.
(A) Co-immunoprecipitation of Flag-tagged Pol3, the catalytic subunit of Polδ, with PCNA during normal growth or in the presence of MMS. No significant change of association is detected with the K20Q or the K77Q mutants. **(B)** Coomassie stained gel showing the different purified PCNA proteins used for *in vitro* DNA-synthesis assays (Figures 6B). *In vitro* DNA synthesis assays using indicated PCNA proteins loaded on DNA by RFC to stimulate the activity of Polη **(C)** or Polζ **(D)** TLS polymerases. Extension of 32P-labelled primer by TLS polymerases was allowed for the indicated times and analyzed on denaturing gels followed by autoradiography. Wild type, K20Q and K77Q mutant PCNA molecules stimulate DNA synthesis to the same extent. **(E)** Model of how the extension has been quantified. The assay gel (example shown here is from Fig. 6D) was divided in four blocks (I to IV) and intensities of radioactive signals were quantified by BioRad Quantity-One software. The product of each block was quantified and expressed as the % of the products in the entire labeled DNA in the lane. **(F)** Quantification of the polymerase assay using recombinant Pol30-WT and Pol30-K20ac with Polδ in Figure 3E. **(G)** Quantification of the polymerase assays using Polδ and the different PCNA mutants. **(H)** Quantification of Polη extension by the different PCNA mutants.

Supplemental Figure S6. **The effect of K20ac on the structure of α1, β8-loop J-β9 and the K164-containing loop,** related to Figure 7.
Overall structure of PCNA surrounded by zoomed views of omit maps for regions of biological importance. Omit maps of acetylated **(A)** and unacetylated (PDB ID 5JNE, Streich et al. Science 2016)**(B)** K20. Composite omit maps of K20 on $PCNA^{K20Ac}$ was contoured at 1.5σ and rendered in blue. This region of PCNA is shown in stick model in which carbon, oxygen and nitrogen atoms are colored in green, red and blue respectively for $PCNA^{K20Ac}$ while the carbon atoms of unacetylated PCNA are highlighted in orange. A potential hydrogen bond is also shown as a red dash line. **(C)** Omit map surrounding β8 and β9 demonstrating a good correlation between the final model and the initial electron density map. The map is contoured at 1.5σ in blue and carbon, oxygen and nitrogen atoms are colored as in A. The lack of electron density for residues 108-110 in the loop J connecting the β sheets is observed. Also shown is a zoomed view on Y114 indicating that the side chain of this residue can be unambiguously modeled in the map. **(D)** Acetylation of K20 does not significantly impact the movement of PCNA K164 SUMOylation site. Shown is a composite omit map of the K164-containing loop of PCNA-K20ac. Owing to the lack of electronic density of K164 side chain, the residue was modeled as an alanine. The omit maps were generated using the Phenix software.

Supplemental Figure S7. FACS analysis of the cell cycle progression of Pol30-K20Q and Pol30-K20A mutants, their growth in the absence of NER and BER repair pathways, and model of DNA damage tolerance pathways in relation to different post-translational modifications of the PCNA ring, related to Figures 5, 6 and 7.
(A) The progression of Pol30-K20Q and Pol30-K20A mutants in S phase upon MMS exposure was monitored. Cells were synchronized in G1 and released in S phase with 0.02% MMS. The analysis of DNA content was monitored by FACS analysis every 30minutes. **(B)** Genetic interaction between NER and BER repair genes with Pol30-K20Q and Pol30-K20A mutations. **(C)** Model showing the integration of PCNA acetylation by Eco1 at the inner surface of the ring in relation to DNA damage tolerance pathways and known post-translational modifications at its external surface.

Supplemental Table S1.
Acetylated lysines detected on PCNA inner surface in this study and in different large-scale proteomic analysis in eukaryotes. Related to Figure 1.

Supplemental Table S2.
Strains used in this study, related to Figures 1-6.

Supplemental Table S3.
Plasmids used in this study, related to Figures 1-7

SUPPLEMENTAL TABLES

Supplemental Table S1.
Acetylated lysines detected on PCNA inner surface in this study and in different large-scale proteomic analysis in eukaryotes. Related to Figure 1.

Lysine position	Alpha helix	Organism	Reference
13	1	Rattus norvegicus (Rat)	(Lundby et al., 2012)
13	1	Saccharomyces cerevisiae (budding yeast)	(Henriksen et al., 2012)
13	1	Homo sapiens (Human)	(Chen et al., 2012)
13	1	Saccharomyces cerevisiae (budding yeast)	This study
13	1	Homo sapiens (Human)	(Cazzalini et al., 2014)
14	1	Homo sapiens (Human)	(Chen et al., 2012)
14	1	Homo sapiens (Human)	(Cazzalini et al., 2014)
20	1	Saccharomyces cerevisiae (budding yeast)	This study
77	2	Homo sapiens (Human)	(Choudhary et al., 2009)
77	2	Homo sapiens (Human)	(Chen et al., 2012)
77	2	Homo sapiens (Human)	(Cazzalini et al., 2014)
80	2	Homo sapiens (Human)	(Choudhary et al., 2009)
80	2	Homo sapiens (Human)	(Chen et al., 2012)
80	2	Homo sapiens (Human)	(Cazzalini et al., 2014)
146	3	Saccharomyces cerevisiae (budding yeast)	This study
217	4	Saccharomyces cerevisiae (budding yeast)	This study
217	4	Saccharomyces cerevisiae (budding yeast)	(Henriksen et al., 2012)

References

Cazzalini, O., Sommatis, S., Tillhon, M., Dutto, I., Bachi, A., Rapp, A., Nardo, T., Scovassi, A.I., Necchi, D., Cardoso, M.C., *et al.* (2014). CBP and p300 acetylate PCNA to link its degradation with nucleotide excision repair synthesis. Nucleic Acids Res *42*, 8433-8448.

Chen, Y., Zhao, W., Yang, J.S., Cheng, Z., Luo, H., Lu, Z., Tan, M., Gu, W., and Zhao, Y. (2012). Quantitative acetylome analysis reveals the roles of SIRT1 in regulating diverse substrates and cellular pathways. Mol Cell Proteomics *11*, 1048-1062.

Choudhary, C., Kumar, C., Gnad, F., Nielsen, M.L., Rehman, M., Walther, T.C., Olsen, J.V., and Mann, M. (2009). Lysine acetylation targets protein complexes and co-regulates major cellular functions. Science *325*, 834-840.

Henriksen, P., Wagner, S.A., Weinert, B.T., Sharma, S., Bacinskaja, G., Rehman, M., Juffer, A.H., Walther, T.C., Lisby, M., and Choudhary, C. (2012). Proteome-wide analysis of lysine acetylation suggests its broad regulatory scope in Saccharomyces cerevisiae. Mol Cell Proteomics *11*, 1510-1522.

Lundby, A., Lage, K., Weinert, B.T., Bekker-Jensen, D.B., Secher, A., Skovgaard, T., Kelstrup, C.D., Dmytriyev, A., Choudhary, C., Lundby, C.*, et al.* (2012). Proteomic analysis of lysine acetylation sites in rat tissues reveals organ specificity and subcellular patterns. Cell Rep *2*, 419-431.

SUPPLEMENTAL EXPERIMENTAL PROCEDURES

Yeast strains, plasmids and site-directed mutagenesis

Yeast manipulations, cultures and transformations were performed according to standard protocols. Gene deletion and tagging was achieved using one-step integration of PCR-amplified modules. Strains used in this study are listed in table 2. All genetic assays were performed using the PY37 strain genotype: MATα *ura3-52 trp1Δ901 leu2-3,112 can1-100 pol30Δ1* + (pBL211 *POL30 URA3*)(Ayyagari et al., 1995b). Cell cycle experiments were performed using the WPY37 strain constructed by mating W303 (MATa) with PY37 (MATα) to generate a MATa strain. These strains (PY37 and WPY37) are deleted for the *POL30* gene but covered by *POL30* WT vector (pBL211 *URA3* auxotrophy). Viability of different mutants expressed from a *TRP1* vector (pBL230) was tested by streaking isolated colonies on 5-FOA. Spot assays represent tenfold serial dilution of mutants on synthetic dropout (SD) plates lacking tryptophan, with or without addition of drugs. The pBL230 plasmid (*TRP1 CEN6 ARSH4 POL30*-WT) was used for phenotypic analysis, which expresses the *POL30* gene under its endogenous promoter and terminator (see tables 2 and 3 for list of strains and plasmids). Mutations were introduced by PCR with one oligonucleotide containing the mutation by the high fidelity Phusion polymerase (Thermo Scientific) following the conditions: initial denaturation (96°C, 1min); 25 cycles of denaturation (98°C, 10sec), annealing (60°C, 20sec), extension (72°C, 4min 30sec) and final extension (72°C, 7min). Upon completion, PCR reactions were digested by Dpn1 for 2 hours at 37°C and transformed into bacteria. All mutations were confirmed by DNA sequencing. For overexpression experiments and PCNA purifications, the ORF and terminator of *POL30* were cloned into 2Flag-pFL36 plasmid containing the PGK promoter.

Drug sensitivity assays

Yeast strains were grown overnight at 30°C to stationary phase in Trp- SD medium, then diluted to an optical density (O.D) of 0.2 at 600nm and further incubated for 5hrs. Tenfold serial dilutions of cycling yeast were spotted onto solid medium containing indicated concentrations of drugs or DMSO for control. Plates were incubated at 30°C, unless otherwise indicated, for 2-4 days. For survival assays in liquid culture, exponentially growing cells were treated with 0.2% MMS for the indicated time and plated at a concentration of about 100cells/plate. Colonies were counted after 2-4 days.
In order to measure the viability in G1 and S phases, cells were first synchronized in G1 with 14μM alpha factor for 2hours and then either directly treated with 0.03% MMS for 2 hours or released in S phase in media containing 0.03% MMS for 2 hours, for G1 or S phase treatment respectively. After treatment, cells were washed in 2.5% sodium thiosulfate to inactivate the MMS and plated at a concentration of about 100 survival cells/plates.

Antibodies

The antibodies for western blotting were used in 1% milk in TBS-tween 0.1% at the following dilutions, unless otherwise indicated: anti-Flag M2-HRP (1/10000, Sigma); anti-acetylated-Lysine K2-100#9814 (Cell Signaling technology), anti-PCNA (gift of H.

Ulrich, 1/2500), anti-PCNA (1/2500, ab70472), anti-K20Ac (1/2500) and anti-His (1/2500, Clontech).

Acetyl-lysine immunoprecipitation

Endogenously Flag-tagged PCNA-expressing cells were synchronized in G1 phase using 7µM α-factor for 2hours and released in S-phase for 2hrs in media containing the indicated drug, or for 15minutes in YPD alone. Cells were harvested and resuspended in lysis buffer (10mM Hepes pH7.5, 350mM NaCl, 10% glycerol, 0.1% Igepal, 1% SDS, 2% Triton X-100, 2µg/mL, leupeptin, 2µg/mL pepstatin A, 5µg/mL aprotinin, 1mM PMSF, 10mM β-glycerophosphate, 10mM Na-Butyrate, 0.5mM NaF, 1mM DTT, 2,5mM MgCl2, 0.5mM CaCl2, 25mM Nicotinamide and 10µg/mL TSA) then mechanically disrupted using glass beads at 4°C with a vortex. To solubilize DNA-bound proteins, lysate was digested using 10U DNAse I (NEB) for 1 hour on ice. Each IP were performed using 1mg of total extract. The acetylated-fraction was captured using acetyl-lysine antibody (antibody K-103, Cell signaling). 4µL of acetyl-lysine antibody was prebound to beads by incubating for 4 hours with protein-A sepharose and then added to the extract for overnight incubation at 4°C. Beads were abundantly washed in the wash buffer (10mM Hepes pH7.5, 350mM NaCl, 0.1% Igepal). Captured material was analysed by western-blot using Flag-HRP antibody (1:1000) incubated overnight at 4°C.

Production of K20Ac antibody

Rabbit polyclonal antibody against PCNA K20Ac was produced and purified by Médimabs. The animal was immunized with a chemically acetylated peptide IIDGF**K**(ac)DSVQLDC corresponding to the yeast Pol30 sequence surrounding K20. In order to avoid a possible chemical modification of the cysteine residue (C) during manipulation of the peptide, the C from the normal sequence was substituted for the sterically equivalent amino acid serine (S). However, the antibody purification was performed using both K20-acetylated and non-acetylated peptides corresponding to Pol30 native sequence. Enriched antibody (790µg/mL) was validated on ELISA using both acetylated and non-acetylated peptide.

2D-gel electrophoresis

For the first separation IPG (Immobilized pH gradient) strips were rehydrated overnight at 20°C in Rehydratation Buffer (8M urea, 1% CHAPS, 15mM DTT) containing the sample in the Immobiline DryStrip pH4-7 7cm (Amersham Biosciences). Isoelectrofocusing was performed at 20°C at 20,000V/h. Strips were washed for 10min in Wash Buffer 1 (6M urea, 2% SDS, 375mM Tris pH8.8, 20% glycerol and 65mM DTT) and 10min in Wash Buffer 2 (6M urea, 2% SDS, 375mM Tris pH8.8, 20% glycerol and 135mM iodoacetamide). After washes the second migration was performed using a standard 12% SDS-PAGE.

Protein purifications and PCNA modifications

DNA polymerases, RPA and RFC were prepared as described previously (Li et al., 2013). PCNA mutants and NuA4 complex (Epl1-Flag) were purified from yeast through the Flag epitope following standard procedures. Briefly, purification was done from 1L culture lysed with glass beads in lysis buffer (10mM Tris-HCl pH8.0, 270mM NaCl, 0,1% NP40, 10% glycerol, 0.5mM DTT, 1mM PMSF, leupeptin, 2µg/mL pepstatin A,

5µg/mL aprotinin, 5mM β-glycerophosphate, 5mM sodium butyrate). Insoluble material was removed by centrifugation at 14000rpm for 30min and an ultracentrifugation at 45000rpm for 45min. After a preclear of 1 hr at 4°C using CL-6B sepharose (Sigma), immunoprecipitation using anti-Flag M2-agarose beads (Amersham) was performed overnight at 4°C. After abundant washes in lysis buffer (500mM NaCl), tagged proteins were eluted with 150µg of 3xFlag peptide in Flag Buffer (10mM Tris HCl pH8.0, 100mM NaCl, 0.1% NP40, 10% glycerol, 0.5mM DTT, leupeptin, 2µg/mL pepstatin A, 5µg/mL aprotinin) for 2hours at 4°C. Recombinant His-Eco1 was expressed in *E. coli* BL21 Codon Plus (DE3)-RP and purified on Ni-NTA resin according to standard procedures. Briefly, after IPTG induction, cells were harvested by centrifugation, washed in 20mM Tris-HCl pH7.5, 200mM NaCl and lysed in 20mM Tris-HCl pH7.5, 400mM NaCl, 0.5% Igepal, 2% Triton X-100, 1mM PMSF with 0.3mg/mL lysozyme and sonication. The supernatant was cleared by centrifugation at high speed at 4°C and incubated with Ni-NTA beads supplemented with 20mM imidazole pH7.0. After 1hour incubation, beads were abundantly washed in high salt buffer and eluted with 500mM imidazole. In addition, Eco1 was dialyzed in the Flag buffer overnight at 4°C. Recombinant Rtt109-Vps75 complex was purified from bacteria as previously described (Tang et al., 2011).
To determine the level of SUMO modifications of PCNA in the Pol30-K20Q mutant we used a plasmid expressing His-PCNA under its endogenous promoter and terminator in the PY37 strain and purified it using Ni-NTA beads in denaturing conditions as described (Davies and Ulrich, 2012).

Expression of PCNA acetylated at single sites
PCNA was expressed in *Escherichia coli* BL21 Codon-Plus (DE3)-RP. Cells were transformed with pCDF PylT and pBKRS-3 plasmids obtained from Jason Chin. A single colony was grown in 500mL LB supplemented with 50µg/mL Kanamycin, 100µg/mL Spectinomycin and 34µg/mL Chloramphenicol at 37°C until the OD600 reached 0.4. At this point, 20mM nicotinamide and 10mM acetyl-lysine was supplemented in the culture for 30minutes. Protein production was then induced by addition of 1mM IPTG and incubated overnight at 16°C. The procedure used to purify His-tagged PCNA was the same than the procedure used for Eco1 purification.

Crystallization and crystal structure determination of acetylated PCNA
Concentrated preparation of purified acetylated PCNA was diluted to 10mg/ml and used to carry out crystallization trials with various sparse matrix screens. Initial hits were obtained with the salt screen (Hampton Research) and further optimized in 24 well plates. Cubic shaped crystals were obtained in 1.0M NH_4SO_4 and 0.1M NaCitrate pH 6.0 by vapor diffusion. The crystals were harvested and transferred into the mother liquor supplemented with 20% glycerol and flash frozen in liquid nitrogen. A complete dataset was collected at the 17-ID-D beamline of LS-CAT (Advanced Photon Source; Argonne National Laboratories). The data sets was processed and scaled using xds and aimless, respectively (Evans and Murshudov, 2013; Kabsch, 2010). A molecular replacement solution was found using Phaser (Zwart et al., 2008) and yeast PCNA structure as a search model (1PLQ.pdb). The model was completed using interactive rounds of refinement and model building using Phaser and Coot, respectively (Emsley et al., 2010).

The model was refined to Rwork/Rfree of 21.3/23.1. The final model includes a proline residue on the N-terminus which corresponds to a portion of the linker region between the histidine tag and PCNA and lacks electronic density for residues 108-110 of protomers A and B while residues 105-110 are missing in protomer C. Finally, owing to the lack of electron density, K164 of the B and C molecules was removed from the model. This crystal structure has been deposited to the protein databank (PDB ID **5T9D**). The final model contains no Ramachandran outliers and shows good geometrical statistics with a Molprobity score of 1.73.

***In vitro* acetyltransferase assay**

Acetyltransferase assays with 500ng of purified PCNA and 0.5, 1 or 2µg of recombinant Eco1 were performed in a 15uL reaction with 400µM of cold AcCoA in HAT buffer [50mM Tis-HCl pH 8.0, 50mM NaCl, 0.1mM EDTA, 5% glycerol, 1mM DTT, 1mM PMSF, 10mM sodium butyrate] at 30°C during 6 hours. Samples were loaded on 12% SDS-PAGE gels for detection by Western blot. Rtt109/Vps75 and NuA4 activities were tested on core histones with cold and radioactive AcCoA while Eco1 activity was measured through auto-acetylation.

DNA polymerase assay

Details of the in vitro reconstituted system, purification of the different factors and details about the reactions were described previously (Li et al., 2013). Bluescript SK-ssDNA (10nM) was hybridized with 10nM of the 70-mer oligonucleotide (TSO236) that was labelled with 32P, and incubated with RPA (1.1µM), RFC (30nM) and PCNA (200nM) for 3 min at 37°C. DNA synthesis was started by adding Polδ (16nM) and products were analysed by electrophoresis through 8% polyacrylamide gel containing 8 M urea.

Mass spectrometry analysis and acetylation site detection

Purified proteins to be analyzed were resolved on 12% SDS-PAGE gel and in-gel digested with the trypsin or chymotrypsin protease as was previously described (Lambert et al., 2010) and stored at -80°C until analysis. Five microliters of the digested peptides (corresponding to half of the total sample) was used per analysis. To do so, a homemade spray tip of a fused silica capillary column (0.75 µm inner diameter, 350 µm outer diameter) was packed with 10 cm (±1 cm) of C_{18} reversed-phase material (Reprosil-Pur 120 C18-AQ, 3 µm) packed in the column with a pressure bomb. The column was then pre-equilibrated in buffer A before being connected in line to a NanoLC-Ultra 2D plus HPLC system (Eksigent) coupled to a LTQ-Orbitrap Elite (Thermo Electron) equipped with a nanoelectrospray ion source (Proxeon Biosystems). The LTQ-Orbitrap Velos instrument under Xcalibur 2.0 was operated in the data-dependent mode to automatically switch between MS and up to 10 subsequent MS/MS acquisitions. Buffer A is 100% H_2O, 0.1% formic acid; buffer B is 100 ACN, 0.1% formic acid. The HPLC gradient program delivered an acetonitrile gradient over 125 min. For the first 20 min, the flow rate was of 400 µL/min at 2% B. The flow rate was then reduced to 200 µL/min, and the fraction of buffer B increased in a linear fashion to 35% for 95.5 min. Buffer B was then increased to 80% over 5 min and maintained at that level until 107 min. The mobile phase was then reduced to 2% B until the end of the run (125 min). The parameters for data-dependent acquisition on the mass spectrometer were 1 centroid MS (mass range

400–2,000) followed by MS/MS on the 10 most abundant ions. General parameters were the following: activation type-CID; default charge state = 2; isolation width = 2 m/z; normalized collision energy = 35; and activation Q = 0.25; activation time = 10 ms. For data-dependent acquisition, minimum threshold was 1,000; the repeat count = 1; repeat duration = 30 s; exclusion size list = 500; exclusion duration = 30 s; exclusion mass width by mass = low 0.03, high 0.03. The resulting .RAW files were saved on a local interaction proteomics LIMS, ProHits, and .mgf files were generated using the ProteoWizard converter implemented within ProHits (–filter "peak- Picking true2"–filter "msLevel2"). The mgf files were searched with Mascot version 2.3 against the Saccharomyces Genome Database (containing 5,834 sequences; released on February 15, 2007), allowing for four missed cleavage sites and acetylation (K and protein N-term), phosphorylation (STY), Gln→pyro-Glu (N-term Q), deamidation (NQ), and oxidation (M) as variable modifications and Carbamidomethyl (C) as a fixed modification. The fragment mass tolerance was 12 ppm (monoisotopic mass), and the mass window for the precursor was ± 0.6 Da average mass. The MS/MS spectrum observed to be acetylated were all manually validated. Images of annotated MS/MS spectra of acetylated peptides (fig. S1) were generated using Scaffold (Proteome Software, inc.). All MS files used in this study, the mascot search results as well as the Scaffold files were deposited at MassIVE (http://massive.ucsd.edu). The MassIVE ID is MSV000078852 and the MassIVE link for download is: http://massive.ucsd.edu/ProteoSAFe/status.jsp?task=bef488e191354bf58633fc76896d92a5. The password for download prior to final acceptance is PCNA2014.

Fluorescence Associated Cell Sorting

WPY37 cells were synchronized in G1 phase with 14µM α-factor for 2hours. Synchronized cells were subsequently washed twice in cold water and released in S phase for the indicated time and treatment. Cell pellet was resuspended in 300µL cold-water and fixed with 70% ethanol overnight at 4°C. Cells were then washed in PBS and sonicated. Samples were incubated with RNase A and propidium iodide. Cell-cycle progression was monitored by flow cytometry (FACS) analysis of DNA content. FACS profiles were generated using the Flowing Software (http://www.flowingsoftware.com/).

References

Davies, A.A., and Ulrich, H.D. (2012). Detection of PCNA modifications in Saccharomyces cerevisiae. Methods in molecular biology *920*, 543-567.

Emsley, P., Lohkamp, B., Scott, W.G., and Cowtan, K. (2010). Features and development of Coot. Acta Crystallogr D Biol Crystallogr *66*, 486-501.

Evans, P.R., and Murshudov, G.N. (2013). How good are my data and what is the resolution? Acta Crystallogr D Biol Crystallogr *69*, 1204-1214.

Kabsch, W. (2010). Xds. Acta Crystallogr D Biol Crystallogr *66*, 125-132.

Lambert, J.P., Fillingham, J., Siahbazi, M., Greenblatt, J., Baetz, K., and Figeys, D. (2010). Defining the budding yeast chromatin-associated interactome. Mol Syst Biol *6*, 448.

Li, J., Holzschu, D.L., and Sugiyama, T. (2013). PCNA is efficiently loaded on the DNA recombination intermediate to modulate polymerase delta, eta, and zeta activities. Proceedings of the National Academy of Sciences of the United States of America *110*, 7672-7677.
Tang, Y., Holbert, M.A., Delgoshaie, N., Wurtele, H., Guillemette, B., Meeth, K., Yuan, H., Drogaris, P., Lee, E.H., Durette, C.*, et al.* (2011). Structure of the Rtt109-AcCoA/Vps75 complex and implications for chaperone-mediated histone acetylation. Structure *19*, 221-231.
Zwart, P.H., Afonine, P.V., Grosse-Kunstleve, R.W., Hung, L.W., Ioerger, T.R., McCoy, A.J., McKee, E., Moriarty, N.W., Read, R.J., Sacchettini, J.C.*, et al.* (2008). Automated structure solution with the PHENIX suite. Methods Mol Biol *426*, 419-435.